~~SECRET~~

[redacted]

[redacted]

COPY NO. [redacted]

VIDYA REPORT NO. [redacted]

December 29, 1964

POST-FLIGHT THERMAL DATA ANALYSIS OF THE "J-7" SYSTEM

by

[redacted]

[redacted]

[redacted]

[redacted]

~~SECRET~~

Logged 23 Feb 65 Filed ✓

[redacted]

TABLE OF CONTENTS

[redacted]

Page
No.

POST-FLIGHT THERMAL DATA ANALYSIS OF THE "J-7" SYSTEM

1. INTRODUCTION

The previous post-flight thermal data analyses of the "J" systems were based upon the assumption that the data obtained from those temperature sensors attached to the vehicle skin were approximately correct. These data contradicted the temperature predictions based upon the assumed orbital thermal environment and the exterior surface thermal paint mosaic. This discrepancy between the analytical and the empirical data was resolved in favor of the empirical skin-temperature data since (1) the thermal environment can have temporal variations whose magnitudes and frequency are unknown and (2) the exterior surface paint mosaic is subject to surface finish degrading effects of unknown magnitude during the launching phase of operation. It is known that there are errors in the skin-sensor data due to the dissipation of electrical energy within the sensors; this was a major source of error for the sensors located within the vehicle. Assuming perfect thermal contact between the sensor and the skin, the relative magnitude of this error depends upon the relative amount of skin sensor electrical heating of the immediate adjacent skin area as compared to the total heat exchange for that particular area. Since the total heat exchange for most skin sensor positions was very large, involving direct solar radiation, albedo radiation, and earthshine radiation, the relative error was assumed to be small. The skin-sensor data for those vehicle areas not exposed to large heat-exchange rates, that is, those always facing dark space can be expected to be somewhat high[1] since the electrical heat input for those sensors become a significant proportion of the total heat exchange for those skin positions.

The vehicle-skin-temperature-sensor data, tape recorded throughout an orbit, were used in previous flights as the thermal boundary conditions to check the thermodynamic consistency of the internal sensor data. The interior components'

[1]The Associate Contractor in a verbal communication October 11, 1963, stated that during a HATS test of an entire system that the skin sensors did not follow the skin temperature as indicated by calibration thermocouples in the low temperature ranges.

[redacted]

temperatures were computed for the thermal environment presented by the vehicle skin as described in Reference 1. With the adoption by the Associate Contractor of the practice of calibrating the temperature sensors for electrical self heating as a function of time prior to flight, the thermodynamic consistency of the sensor data improved considerably. The average variation of the internal temperature data from that computed for the "J-5" system flight was approximately +1° F (Ref. 1, Table II data) while that for the earlier "J-1" flight was approximately +9° F (Ref. 1, Table III data). The flight data, tape recorded through an orbit, were necessary for this type of analysis since the skin temperatures, which vary considerably during an orbital revolution, are used to define an orbital thermal environment for the interior.

The Vidya Division of Itek has not received any tape recorded data for flights "J-9" and "J-7". Following a request of August 27, 1964, to the Associate Contractor by Vidya for the reduction of the "J-7" tape recorded flight data, the Associate Contractor submitted to the customer a cost estimate for that reduction. Vidya was informed September 28, 1964, that the request of the Associate Contractor for funding for the data reduction was denied. The data received, therefore, have been only those acquired at a single orbital position and do not permit a thermal analysis of the previous type since the entire boundary conditions cannot be established.

For the "J-7" post-flight thermal analysis, therefore, it was necessary to assume an average thermal environment due to the solar, albedo, and earthshine radiation heating to which the satellite was subjected during operation. The temperatures expected for various sensors were computed for the assumed thermal environment and for the exterior paint as it was designed. This type of computation can be expected to result in larger differences between the measured and the computed internal temperatures than those for the computations based upon the use of the measured skin temperatures as the

[redacted]

boundary conditions. This is due to the inclusion of additional variables, the unknown variation in the space thermal environment and the unknown variation, if any, in the exterior thermal paint mosaic. Thus, an assessment of the thermodynamic consistency of the internal sensor instrumentation data and the determination of the sources of thermal errors cannot be accomplished as was done for previous flights (Ref. 13 for example). These difficulties with the current data will be explained in detail in subsequent portions of this report.

This report is the last of a series of six thermal analysis reports following the initial "J" system thermal design report. It is appropriate, then, that a résumé be included in this report describing the contributions made by the thermal analyses performed. This résumé is presented in Section 5.

2. METHOD OF ANALYSIS

The data obtained from the Associate Contractor includes the "J-7" system post-flight thermal data as reduced from the telemetered raw data obtained for a single orbital position corresponding to Vandenberg Air Force Base, the paint mosaic design for the "J-7" system, and the orbital β angle as a function of the number of orbital revolutions of the system. This material is presented in Appendix A.

The 130-node mathematical model of the system, together with the resulting solar absorptivity and thermal emissivity of the skin for the designed paint mosaic, were used to compute transiently the system nodal temperatures over an orbital period. The orbital β angle used for these computations was 40° corresponding to the system orbital revolution number 46 (Appendix A). A detailed description of the computational procedure is given in Reference 3. The heat fluxes for the thermal environment at an orbital β angle of 40° were computed by the methods described in Reference 4; for their computation an average terrestrial reflectivity (or albedo constant) value of 0.39 was used for the near polar orbit of the "J-7" system;

the orbital inclination with the equator for this flight was 85° (Appendix A).

The orbital position reference point for the computations was the system's emerging transit of the terminator. In order to relate the transiently computed temperatures to the data acquired at Vandenberg Air Force Base, it was necessary to derive a mathematical expression in terms of the orbital parameters furnished to Vidya for the orbital time required for the satellite to traverse the path from the terminator to the data acquisition station. This derivation is presented in Appendix B.

3. RESULTS OF THE ANALYSIS

A comparison of the in-flight measured temperatures for the vehicle interior as obtained from the data acquired at Vandenberg Air Force Base with the computed nodal temperatures for the nodes, which best approximate the system's temperature sensor locations, is presented in Table I. The flight data utilized for comparison is that for orbits 40 and 47. These orbits have β angles of 40.5° and 39.9°, respectively. The temperature differences resulting from their departure from a β angle of 40° should be less than 1° F in the predictions.[2] The positions on the instruments corresponding to the nodal numbers are presented in the Nodal Breakdown Chart of Reference 1.

A graphical comparison is shown in Figures 1 and 2 for the measured temperatures on the vehicle skin, barrel and fairing, and the model computed temperatures for the orbital position corresponding to the data acquisition station.

4. DISCUSSION OF THE RESULTS

4.1 "J-7" Interior Temperatures

The data comparison shown in Table I indicates an overall average computed interior temperature that is approximately

---

[2] In Reference 1 it is shown that a shift of 53° in β angle produces about a 30° F shift in mean orbital skin temperature. For a linear interpolation this is less than 1° F per degree of β angle shift.

5° F lower than the average of the system interior measured temperatures. By comparison, the temperature level computed for the "J-5" system was within 1° F of the mean of the measured temperatures (Ref. 8). This small difference is expected for the use of measured skin-temperature values as boundary conditions if the interior data is thermodynamically consistent with the skin-temperature data and the thermal behavior of the shielding and interior surface finishes is understood.

Although this agreement to within 5° F between predicted and measured temperatures is quite close considering allowable tolerances of ±10° F about a prescribed mean value, it should not be inferred from these data alone that the mean orbital environmental parameters employed or the skin finish characteristics utilized will always be appropriate. If this were true the agreement to within about 5° F between predictions and actual data should be obtained for each flight. For the purpose of comparing the above results with that for another flight, the flight data for the "J-9" system which had the same external paint mosaic[3] as "J-7" and a similar orbit[4] is compared in Table II. The data presented there are for orbital passes numbers 9 and 16 having β angles of 40.6° and 39.6°, respectively. The equations of Appendix B were used to correlate the orbital position with respect to the terminator for the data with the corresponding computational time in orbit. The predicted temperatures for the data comparison were within 1° F of those computed for the "J-7" flight. The computed temperatures, however, are on the average about 10° F lower than the measured ones. Thus, the "J-9" system average temperature is about 5° F higher than that for "J-7". The differences for the two systems may be due to differing space thermal environments caused by earth-cloud cover variations or they

[3] Communication from the Associate Contractor.

[4] The orbital inclinations were 85° and 80° and the perigee altitudes were 99 N.M. and 84 N.M. for "J-7" and "J-9", respectively. The apogee altitude for "J-7" was 260 N.M.; for "J-9" it was 261 N.M. This information was obtained from the flight report files of the Itek Field Service at A/P.

may be due to variations in vehicle system parameters such as that caused by degradation of surface finishes, variation in instrumentation performance or to data read-out and reduction errors. Also, a combination of the above factors may be responsible.

From the data currently obtained from the "J" systems and the present state of the knowledge of the space thermal environment, the effects of the above two sources, environment and hardware, on temperature variations cannot be separated even approximately. The possible variations of the system mean temperature level due to the temporal variations of earth-cloud cover from its mean can be only roughly estimated until experimental knowledge is obtained concerning the frequency and magnitude of these variations. This estimate is made in Appendix C and indicates that the "expected" variation of system temperature levels for different flights due to "expected" variations of cloud cover is about $+6^{\circ}$ F and -4° F.

These estimated environmentally induced temperature variations might well explain the 5° F difference between the mean-temperature levels of "J-7" and "J-9" assuming, of course, that the variations actually occurred and are not instrumentation errors. However, there exists an approximate 10° F difference in level between the theoretical results and the measured results[5] for "J-9". If there were a strong dependency of the theoretical results upon the absolute value of the assumed mean terrestrial reflectivity, or albedo constant, then a strong possibility would exist for an error in the theoretical value of the mean terrestrial reflectivity

[5] The theoretical results were obtained for the use of a mean solar constant. The actual value of the solar constant during June is smaller than the mean by 3.3 percent. Thus, the actual difference between the theoretical and the measured results should be even greater than 10° F since the computations using a lower heat input to the system would result in a lower mean temperature. All future computations by Vidya Division of this type will include the value of the solar constant existing for that flight date.

used in the computations. However, it is shown in Appendix D that for the "J" systems in an orbit having $\beta = 40^{\circ}$, the mean orbital temperature of the satellite is almost completely independent of the magnitude of the mean or long term value of the terrestrial refelctivity; only temporal variations in the terrestrial reflectivity cause temperature variations. Thus, the hardware parameters or perhaps the data itself must also be suspected as contributing to the above difference between theoretical and measured temperatures. There can be no definite conclusions reached by these arguments, however, since the estimated variations in the mean orbital temperature due to temporal cloud-cover variations are merely estimates. Therefore, as stated above and now rephrased for emphasis, the present dearth of knowledge concerning the frequency and magnitudes of variations in the amount of earth-cloud cover prevents the separation of the causes of satellite temperature deviation from the designed-for value into those causes due to the environment and those due to the actual hardware. The separation of these causes requiresthe experimental determination of the frequency and magnitude of the variations in the extent of cloud cover. If these variations are found to be larger, then the separation of these causes requires the monitoring of the space thermal environment existing for each flight either by the means of devices aboard each "J" system or of a separate, relatively long-life satellite, especially designed for this one task, having approximately the same orbital inclination as that of the "J" systems. A stronger incentive for the improvement of passive thermal control techniques may result if it were shown that the temperature variations from the expected values now experienced by the "J" systems are not due solely to the variations of the space thermal environment from flight to flight. On the other hand, if the variations in the space-thermal environment are shown to be the source of the thermal control difficulties then any improvement in

the temperature control will require the use of active thermal control methods.

4.2 "J-7" Skin Temperatures

The graphical comparison of the computed skin temperatures with the measured skin temperatures for the orbital position corresponding to the data acquisition station is presented in Figures 1 and 2.

Qualitatively, these results are about what can be expected for the present model and the current hardware sensor instrumentation. The computed barrel temperatures for the sun side are expected to be somewhat lower than the measured values for a daylight pass over the data acquisition station for the reason explained in Appendix H. It would follow from this same reasoning that the computed temperatures for those same nodes should be higher than the measured values during a night pass; however, the electrical self heating of the skin sensors, discussed in the Introduction, will dampen the rate of the indicated temperature drop during the night pass[6]; consequently, the measured results are probably high.

For the fairing section, the conical section, the computed temperatures are expected to differ from the measured ones, but without specifically including the first recovery unit in the mathematical model the algebraic sign of the difference cannot be predicted. The explanation for this is also presented in Appendix H.

For the cold side of the vehicle, the side not exposed to direct solar radiation and for the opposite side as well during the night pass, the measured temperatures are higher than the computed ones as shown in Figures 1 and 2. The probable reason for this is that given above and, also, previously in the Introduction with the supporting statement of the Associate Contractor (Footnote 1); namely, the electrical self heating of the skin-temperature sensors introduces a

[6]During the daylight pass this self heating will accelerate the indicated temperature rise, but the total heat exchange rate due to the direct solar radiation is of such a greater magnitude that the effect of the sensor self heating is negligible by comparison.

a positive temperature error in the data for the low temperature ranges.

The above discussed differences between the computed, instantaneous, transient temperatures and measured temperatures at the single, satellite orbital position shown in Figures 1 and 2 are of a magnitude of from 0° to 30° F. The amplitude of the skin's transient temperature over an orbital period is from Figure 1 about 80° F; this is the difference between measured, instantaneous temperatures at a body angle of 60° for the day and night passes for the data acquisition station position. From the 35 percent error in temperature amplitude expected, discussed in Appendix H, p. H-3, an error of about 30° F could be expected in the computed temperatures. Also, in Appendix H it is shown that this error in the computed instantaneous skin temperature results in an error of only about 1° F for the interior temperatures. Thus, the errors in the computation of the transient, skin temperatures result in a negligible error in the computed interior temperatures.

The effects of the variation of cloud cover as discussed above in Section 4.1 will apply to the exterior transient temperatures also.

5. RÉSUMÉ OF THE CONTRIBUTIONS TO THE "J" PROGRAM RESULTING FROM THE THERMAL ANALYSES

5.1 Thermal Design

The thermal design analyses performed by Vidya Division in liaison with the Associate Contractor resulted in a passive thermal control design for the system that would permit system operations at any orbital β angle. With this design, an interior temperature between 70 and 80° F should be maintainable for any β angle (Ref. 1, Table V).

To attain this performance it is necessary to employ a radiation shield liner having a thermal emissivity of about 0.12. It is required that the mean orbital skin temperatures of the vehicle at a $\beta = 53°$ be about 110° F. This was pointed out explicitly in the original design report on page 6 of Reference 1. Quoting from that page, "... the best instrument temperature ranges are experienced with a nominal skin temperature of 110° F." The underlined portion is underlined in the original text.

Unfortunately, the thermal radiation shield fabricated for the system, as measured by the Associate Contractor, had an emissivity between 0.2 and 0.4. The variation of thermal performance with the numerical value of this emissivity is nonlinear; the mean value of the emissivity, 0.3, is completely inadequate to provide the required shielding. Computations made by Vidya Division using the 130-node mathematical model show that this shield is but little more effective in providing the desired thermal performance than a black shield would be (Ref. 13, Section 5.1).

For flights more recent than the "J-7" system flight a new radiation shield has been incorporated. This shield appears visually to have a lower thermal emissivity than the value 0.3 described above. However, for the flight thermal results for the first two systems containing this shield as reported qualitatively to Vidya Division, it appears that the designed mean orbital vehicle skin temperature was not in the

required 110° F range at a $\beta = 53°$, but was much lower instead. The resulting interior temperatures as indicated by the flight data (again, a qualitative report to Vidya Division) were low, in the 45° F range. This kind of result can be expected to be obtained in the future unless the original design philosophy of maintaining high mean skin temperatures is followed[7].

5.2 Post-Flight Thermal Data Analyses

An important contribution to the thermal performance of the "J" systems has been the improvement in the accuracy of the interior temperature sensor data.

Originally, the Associate Contractor noted that, during ground tests, variations as a function of time occurred in the temperatures as indicated by the interior sensors. A test was then performed by the Associate Contractor using a sensor attached to a metal honeycomb specimen and from the temperature-time history data resulting from this test, a calibration curve was obtained to correct the flight data (Ref. 11). Vidya Division also performed a test of a sensor attached to a metal honeycomb specimen having different dimensions from that used by the Associate Contractor (the same type of honeycomb material was used as that used in the fabrication of the instrument main plates). A different temperature-time history for the sensor was obtained by Vidya as compared to that obtained by the Associate Contractor. A mathematical model

[7] In a recent verbal communication from the Associate Contractor, information was received that the third "J" system having the new low emissivity radiation shield had, in flight, an interior temperature of about 70° F. Also the information relative to the external paint mosaic was that the sun side of the vehicle had an α/ϵ of about the same numerical magnitude as for the previous systems ($\approx$ 1.1) and the shadow side of the vehicle on the side not exposed to the sun was entirely gold covered. An approximate computation by Vidya Division for this thermal mosaic indicates that a mean orbital skin temperature of about 105° F should have been obtained at $\beta = 53°$. Thus, the thermal design for the most currently flown system (circa January 1965) appears to be in line with the original design philosophy. The question remains, however, of why it was necessary to use a trial-and-error method by which the two previously flown systems in which low emissivity shields were employed ran cold, to obtain the thermal design described one and one-half years ago in Reference 1?

of the sensor as attached to a metal honeycomb structure was used to analyze the test results. This analysis revealed that the two tests, Vidya Division's and the Associate Contractor's, were equivalent, the difference between them being introduced by the specimen dimensions used. The basic information obtained from this analysis was that one single sensor calibration could not be used for the system because the amount of sensor self heating was dependent upon the sensor's position on the instruments. The Associate Contractor then began individual sensor calibration in situ during the vacuum chamber tests prior to flight.

The improvement in the accuracy of the interior sensor data is illustrated by the previously reported (page 2 of this report) decrease in the magnitude of the measured temperature level variation from that predicted from thermodynamic principles.

A continuing flight to flight monitoring of the interior sensor data was conducted by comparing them with the results of the 130-node mathematical model. The measured skin sensor data were used as boundary conditions to ascertain the consistency of the internally measured results with thermodynamic principles. For each flight for which the measured skin data were obtained the results were compared in tabular form, as for example, Tables I and II of this report. The purpose of this monitoring was to provide an independent quality check upon the measured data and thermal performance of the instrument. This is indispensible for a new system since there are nearly always some initial system flaws that must be corrected. The above described temporary correction for sensor self heating (a new system of sensor instrumentation is necessary for a basic correction) is an example of the use of an independent monitoring of the data for the initial break-in period of a new system. Also, this has resulted in an effort to obtain continuity from the initial thermal design effort through this break-in period.

The written reports for this monitoring function are usually quite late in time compared to the system flight schedules. The contents of the reports are not the entire fruits of the work, however, the liaison activity between the two Associate Contractors to improve the system constitutes a large part of the results.

Once the flaws in a new system have been revealed the flight to flight monitoring of the data is no longer necessary. Thus, Vidya does not recommend a continuation of this effort on a routine basis. It is recommended, though, that when changes are made in the internal thermal control surfaces or in the sensor instrumentation that an independent check of the flight data by Vidya be made for the flight of the system in which the changes were incorporated.

Other relatively short-term tasks performed during these post-flight data analyses by Vidya have been the following:

a. An analysis of the thermal effects of air bubbles in the cement used to attach the sensors to the instrument (Ref. 1). (The effects were found to be detrimental to sensor accuracy and a recommendation was made to Itek that tighter quality control be employed in the attachment of the sensors.)

b. An analysis of the effects of the transient exposure of the lens to the exterior environment during operation (Ref. 2). (The resulting temperature changes were found to have a negligible effect upon record quality as measured by the image shift from the record.)

c. An analysis of the effect of temperature level upon record quality (Ref. 2). (This analysis required the use of detailed temperature histories, the tape recorded flight data, for several flights. The detailed thermal data reduction was discontinued beginning with the "J-9" system and this analysis procedure was aborted.)

6. CONCLUSIONS

It is concluded from the results of the analyses of the "J-7" and "J-9" systems that

a. The differences between the mean of the measured temperatures and the mean temperatures computed by Vidya Division for the solar constant's value existing at a given flight date for the "J" systems are due either to temporal variations in the space thermal environment or to variations in the values of the hardware design parameters.

b. In order to evaluate numerically the relative effects of the two causes (Item a above) of the variations in a satellite's thermal performance, it is necessary to determine the magnitude and frequency of the variations in the space thermal environment and possibly to monitor the space-thermal environment during each flight.

c. Should the necessity arise to improve the accuracy of the transient temperature computations for the vehicle skin it will be necessary to increase the number of nodes in the mathematical model to include the skin reinforcing structures as separate nodes.

From the thermal analyses of the first six-system flights it is concluded that[8]

a. The temperature sensor instrumentation should be changed to eliminate the necessity of individual sensor self-heating calibrations[9].

---

[8]At the current date (February 1965) the emissivity of the internal radiation shield of the vehicle is on the order of that specified in the initial design report, therefore, these are conclusions not concerning the shield.

[9]In Reference 2, Section 3.3, it is pointed out that the calibrations change as a function of the environmental temperature level; hence, calibrations at one level used for system temperatures at different levels will result in data errors.

b. Air bubbles should be entirely eliminated from the temperature sensor cement (Ref. 13).

c. Greater accuracy in the computation of the internal temperature distribution of the system requires a more detailed nodal breakdown (more nodes), experimentally measured values of the thermal contact resistance across riveted and bolted structural joints, the experimentally measured values of the specular reflectivities of the different surface finishes, and the inclusion of the specular nature of the surface finishes in the computations[10].

d. A post-flight thermal data analysis is not necessary for each future flight of the "J" systems. Periodical analyses should be made however to assure the maintenance of quality control in data acquisition (instrumentation plus data readout and reduction). Also, the results of new sensor instrumentation and new interior surface finishes should be checked by an analysis of the flight results.

From the flight results to date (circa February 1965) and the indications that a period of one and one-half years has been required to attain in the hardware the initially specified design properties for the "J" system, it is concluded that there is considerable room for improvement in the quality of the liaison between design groups and operations groups.

7. RECOMMENDATIONS

The recommendations based upon the conclusions of Section 6 are as follows:

a. That the magnitude and frequency of the variations in the space-thermal environment of the "J" systems be measured experimentally.

---

[10] All of these items need not be accomplished simultaneously to improve the accuracy; for example, the increase in the number of nodes will in itself increase the accuracy as explained in Appendix H of this report.

b. That the type of temperature sensor instrumentation existing in the systems through "J-7" should be replaced with instrumentation that eliminates the sensor self-heating error.

c. That post-flight thermal data analyses be made for perhaps only one in ten future flights for the purpose of maintaining an independent check upon the quality of the flight data and thermal design.

d. That post-flight thermal data analysis be made for the flight of a system in which new temperature sensor instrumentation or new internal surface finishes are employed. This analysis should be performed as soon as possible after such a flight in order to permit its results to be applied to the design of the immediately succeeding flight.

e. That post-flight thermal data analyses be performed for any flight for which abnormal thermal performance is suspected from the thermal data.

REFERENCES

1. [redacted]

2. [redacted]

3. [redacted]

4. [redacted]

5. Danjon, Andre: Albedo and Color of the Earth, The Earth as a Planet. Edited by C. P. Kuiper, University of Chicago Press, 1954.

6. Handbook of Geophysics. MacMillan Company, New York, 1960.

7. Basic Studies on the Use and Control of Solar Energy. Annual Report NSFG 9505, August 1959 - August 1960, UCLA.

8. Johnson, J. C.: Physical Meteorology: MIT and John Wiley and Sons, Inc., New York, 1960.

9. Smithsonian Physical Tables. Ninth Revised Edition, Smithsonian Institution, Washington, D. C., 1959.

10. [redacted]

11. [redacted]

12. [redacted]

13. [redacted]

[redacted]

TABLE I.- COMPARISON OF "J-7" FLIGHT DATA WITH COMPUTATION RESULTS.

System Sensor	Approx. Node Number	DAY PASS			NIGHT PASS		
		T_S Orbit # 47	T_M Computed $\beta = 40^\circ$	ΔT $T_M - T_S$	T_S Orbit # 40	T_M Computed $\beta = 40^\circ$	ΔT $T_M - T_S$
1-I-3	59	50° F	55° F	+5° F	49° F	56° F	+7° F
1-I-4	42	54	52	-2	59	53	-6
1-I-5	61	57	59	+2	59	60	+1
1-I-6	56	69	63	-6	73	64	-9
1-I-7	52	65	60	-5	66	60	-6
1-I-8	61	61	59	-2	63	60	-3
1-I-9	60	67	63	-4	71	63	-8
1-I-10	52	66	60	-6	64	60	-4
1-I-11	16	66	57	-9	64	57	-7
1-I-12	59	51	55	+4	52	56	+4
1-I-13	15	68	58	-10	70	57	-13
2-I-3	70	76	62	-14	76	62	-14
2-I-4	47	72	69	-4	74	60	-14
2-I-5	72	65	58	-7	66	59	-7
2-I-6	67	60	55	-5	61	56	-5
2-I-7	63	65	57	-8	63	57	-6
2-I-8	72	58	58	0	67	59	-8
2-I-9	71	55	53	-2	58	54	-4
2-I-10	63	66	57	-9	64	57	-7
2-I-11	37	57	58	+1	61	56	-5
2-I-12	70	72	62	-10	72	62	-10
2-I-13	36	64	55	-9	66	55	-11
SP.-1	75	54	59	+5	57	60	+3
SP.-2	75	60	59	-1	63	60	-3
CL.-1	74	70	68	-2	72	72	0
CL.-2	74	72	68	-4	75	72	-3

T_S measured temperature

T_M computed, model nodal temperature

TABLE II.- Comparison of "J-9" Flight Data with Computation Results.

System Sensor	Approx. Node Number	DAY PASS			NIGHT PASS		
		T_S Orbit # 16	T_M Computed $\beta = 40^\circ$	ΔT $T_M - T_S$	T_S Orbit # 9	T_M Computed $\beta = 40^\circ$	ΔT $T_M - T_S$
1-I-3	59	55° F	55° F	0° F	57° F	56° F	-1° F
1-I-4	42	62	52	-10	63	53	-10
1-I-5	61	67	59	-8	68	60	-8
1-I-6	56	75	63	-12	79	64	-15
1-I-7	52	76	60	-16	79	60	-19
1-I-8	61	69	59	-10	72	60	-12
1-I-9	60	71	63	-8	76	63	-13
1-I-10	52	73	60	-13	72	60	-12
1-I-11	16	75	57	-18	72	57	-15
1-I-12	59	57	55	-2	59	56	-3
1-I-13	15	77	58	-19	79	57	-22
2-I-3	70	74	62	-12	74	62	-12
2-I-4	47	71	69	-2	73	60	-13
2-I-5	72	65	58	-7	68	59	-9
2-I-6	67	61	55	-6	62	56	-6
2-I-7	63	68	57	-11	68	57	-11
2-I-8	72	63	58	-5	64	59	-7
2-I-9	71	57	53	-4	58	54	-4
2-I-10	63	74	57	-17	70	57	-13
2-I-11	37	58	58	0	60	56	-4
2-I-12	70	66	62	-4	68	62	-6
2-I-13	36	72	55	-17	73	55	-18
SP.-1	75	53	59	+6	55	60	-15
SP.-2	75	61	59	-2	62	60	-2
CL.-1	74	75	68	-7	71	72	+1
CL.-2	74	73	68	-5	69	72	+3

T_S measured temperature

T_M Computed, model nodal temperature

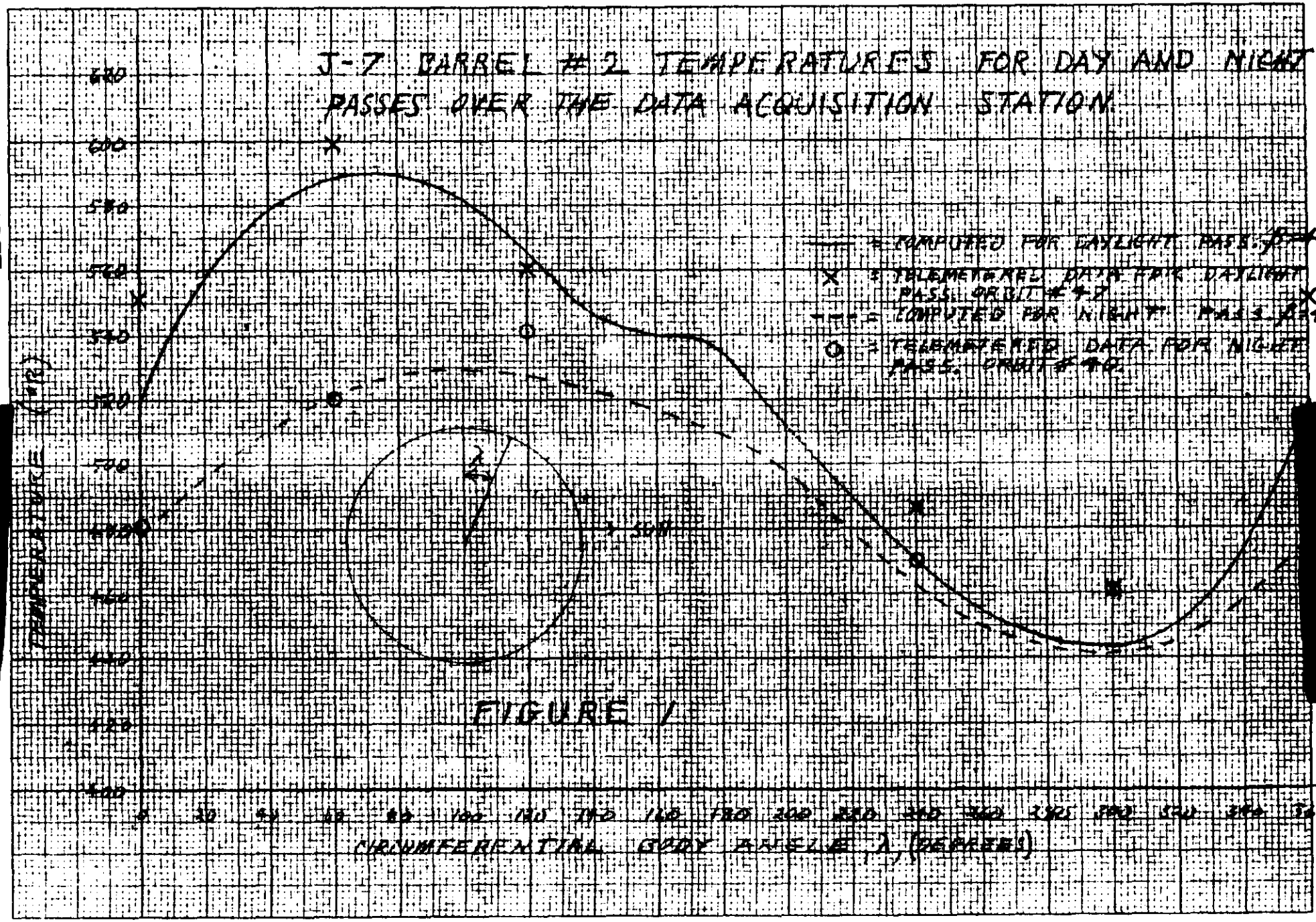

FIGURE 1

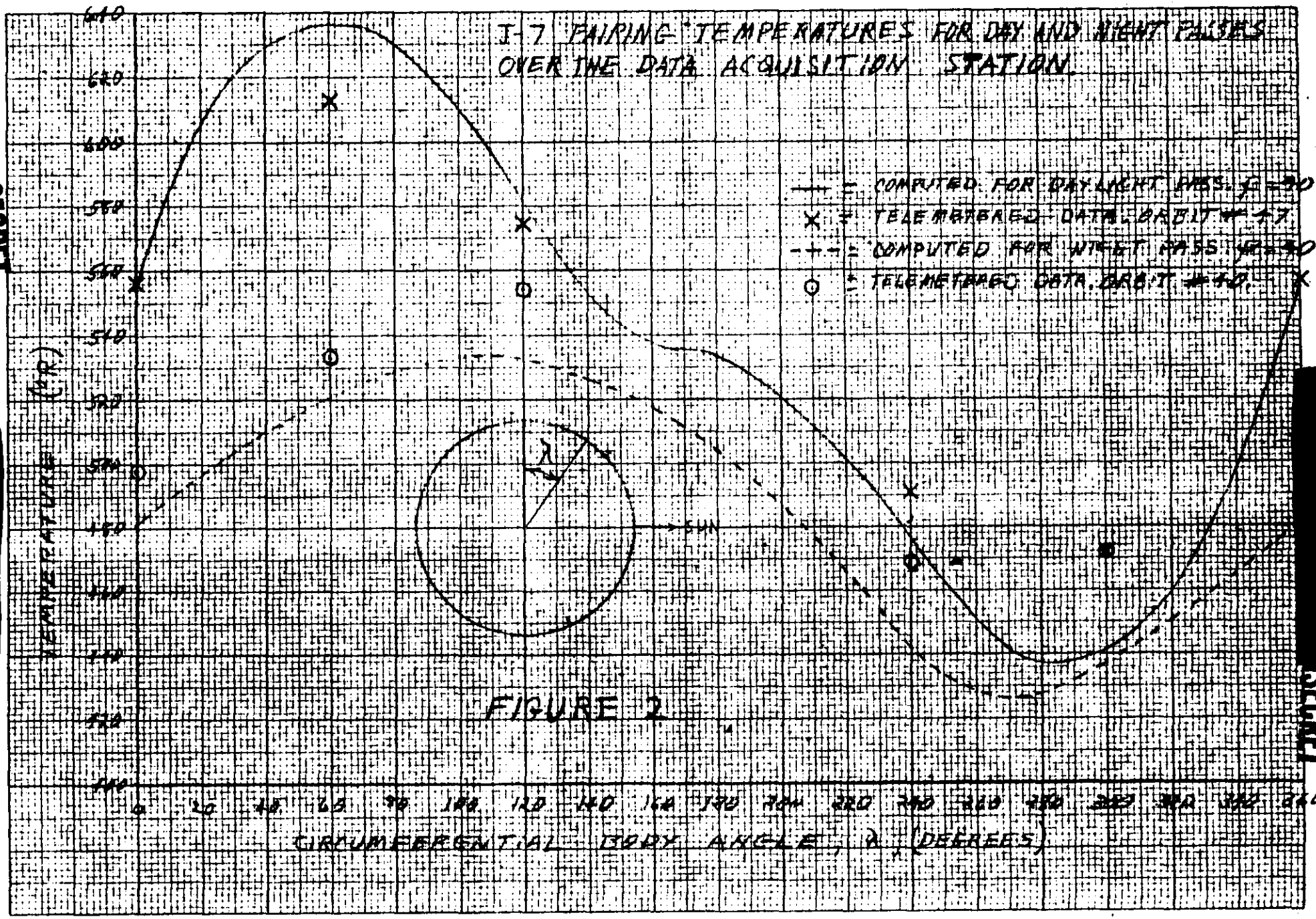

FIGURE 2.

[redacted]

APPENDIX A

THE "J-7" SYSTEM POST-FLIGHT DATA RECEIVED FROM THE ASSOCIATE CONTRACTOR

[redacted]

SEP 28 1964

[redacted]

SECTION

ORBIT

Master	1	8	16	24	31	40	47	56	63	71	79	87	94	103	110	119
3	69	54	49	48	45	49	50	48	45	44	41	44	40	43	45	43
4	73	61	45	54	52	59	54	55	51	50	45	48	45	48	49	47
5	64	63	59	58	54	59	57	58	53	53	48	52	48	52	51	52
6	64	77	71	72	69	73	69	71	65	67	59	66	60	65	62	65
7	64	71	67	65	63	66	65	66	62	60	57	58	57	59	60	59
8	71	67	62	64	59	63	61	62	58	59	53	58	53	57	56	58
9	70	75	68	70	66	71	67	67	63	65	57	57	58	62	60	62
10	69	69	67	63	65	64	66	66	64	59	58	57	58	57	62	58
11	90	66	75	65	70	64	66	64	67	58	60	56	58	55	62	54
12	75	57	52	51	49	52	51	51	47	47	43	46	43	46	47	53
13	71	76	72	70	68	70	68	70	65	63	60	60	59	60	63	59
Slave																
3	67	81	78	75	76	76	76	75	72	71	56	68	68	68	71	67
4	69	77	73	72	71	74	72	73	69	70	64	68	64	68	66	67
5	67	71	66	65	63	66	65	66	62	61	57	59	57	61	61	61
6	63	67	60	60	58	61	60	60	56	57	52	56	52	56	55	56
7	63	71	66	64	63	63	65	63	62	61	57	58	57	58	59	57
8	68	70	64	65	62	67	58	65	61	63	57	61	57	60	59	60
9	67	61	56	57	52	58	55	57	52	53	48	51	49	52	50	52
10	65	71	69	64	66	64	66	66	64	59	60	56	58	56	61	58
11	89	59	58	58	56	61	57	61	57	59	55	56	54	56	57	59
12	70	76	73	70	71	72	72	72	69	69	64	66	63	65	65	66
13	64	69	65	64	62	66	64	66	62	62	57	59	57	58	60	61
Supply Spool																
1	57	72	55	54	53	57	54	57	55	55	54	54	51	53	53	53
2	62	60	61	60	60	63	60	63	60	60	58	58	54	57	57	57

SECRET

SECRET

[redacted]

SECRET

Fairing & Barrel #1	1	8	16	24	31	40	47	56	63	71	79	87	94	103	110	119
1	OBH	38	107	38	99	38	96	38	101	7	23	7	23	7	31	3
2	OBH	15	24	12	18	12	12	12	18	0	0	0	0	0	12	-3
3	OBH	12	-	9	31	9	31	12	28	13	96	10	88	13	104	13
4	OBH	-	-	-	-	-	-	-	-	43	143	40	131	40	142	37
5	OBH	102	132	94	122	94	114	88	113	61	93	55	87	51	95	45
6	OBH	80	177	70	166	73	153	71	160	- - - - - - - F A I R I N G - - - - - - -						
Barrel #2																
1	165	87	115	81	106	81	100	77	99	66	92	58	89	56	94	53
2	150	67	158	61	150	61	139	54	144	51	141	47	130	45	138	41
3	186	21	101	18	99	21	91	21	98	18	90	18	91	18	104	18
4	189	0	10	-2	4	1	1	0	1	-2	-2	-2	-2	-6	9	-2
5	165	10	35	10	26	10	26	10	26	4	20	4	20	4	28	4
Conic Adapter																
1	160	61	100	61	90	61	85	57	87	45	81	43	73	38	81	38
Clock																
1	96	70	75	70	72	72	70	72	72	62	62	62	60	60	65	62
2	101	72	77	72	72	75	72	72	72	64	64	62	62	62	65	62
Thrustcone																
1	OBH	50	50	45	45	46	44	45	43	50	48	48	44	47	47	47
2	84	75	71	68	64	68	63	66	63	64	64	62	63	59	61	59
Stellar Index																
1	96	75	75	72	75	75	72	75	75	72	68	68	68	68	74	68
2	84	72	66	69	69	69	63	69	63	52	45	48	45	45	50	48
Slave Cassette (Recovery System #1)																
1	96	53	45	42	41	44	41	47	46	[redacted]						
Recovery Pattery (Recovery System #2)																
1	71	70	71	65	67	65	65	67	67	78	83	79	78	81	80	81

SECRET

ENCLOSURE #2

[redacted]

[redacted] 19[redacted] SECRET NOV 2 1964 1/4

[redacted]

Ft. 1609 (J-07)

Launch: 4:18 PM EDT ON 19 Dec 1964

Rev 1 i = 85.0°, T = 91 min., h_p = 99 n.m. h_a = 260 n.m.
e = .032

Recovery: Phase A - Rev 65
Phase B - Rev 120

K's

REV	i	GZA	ξ_0	λ_0	λ_0
1	85.0	141°30'	23°26'	5h 54.3m	88°35'
51	85.0	139°12'	23°26'	6h 6.8m	91°42'
101	85.0	136°55'	23°22'	6h 19.3m	94°49'

$\cos\eta = -\cos i \sin\xi_0 + \sin i \cos\xi_0 \sin(GZA - \lambda_0)$

1. $\cos\eta = -(.08716)(.39760) + (.99619)(.91752)(.79776)$
$= -(.03466) + (.72917) = 0.69451$, $\eta = 46°1'$, $\beta = 43°59'$

2. $\cos\eta = -(.08716)(.39768) + (.99619)(.91752)(.73728)$
$= -(.03466) + (.67389) = 0.63923$, $\eta = 50°16'$, $\beta = 39°44'$

3. $\cos\eta = -(.08716)(.39661) + (.99619)(.91739)(.67043)$
$= -(.03457) + (.61310) = 0.57853$, $\eta = 54°39'$, $\beta = 35°21'$

SECRET [redacted]

[redacted]

PAINT PATTERN — FIG. 1559 (J-97)

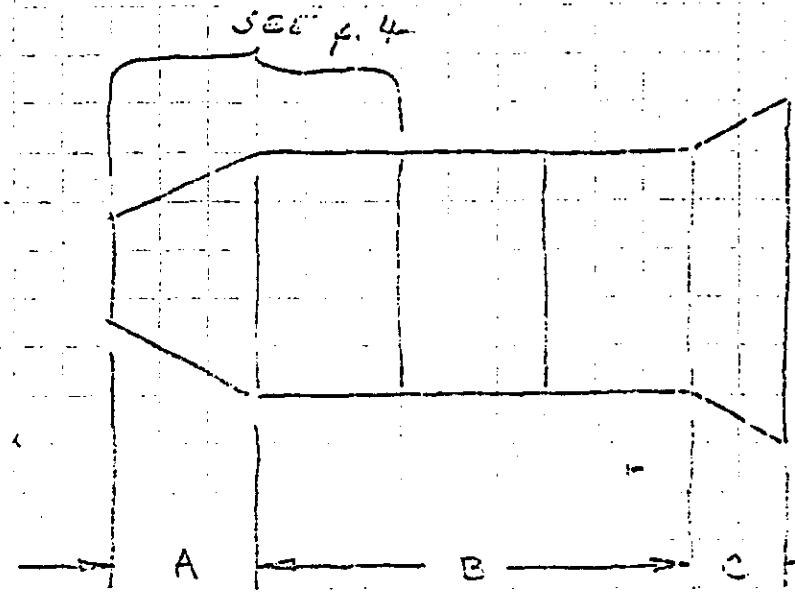

EACH SECTION HAS 42 EQUALLY SPACED (ON 7½° Ø's) LONGITUDINAL STRIPES OF SILICONE SILASTIC EXCEPT AS NOTED ON p. 4.

SECT	STRIPE WIDTH
A	0.50"
B	1.00"
C	0.97"

SILICONE SILASTIC : $\alpha_s/\epsilon = .22/.88$

GOLD : $\alpha_s/\epsilon = .45/.12$

~~SECRET~~

[redacted]

[redacted]

[redacted]

S/C TAPE & PAINT

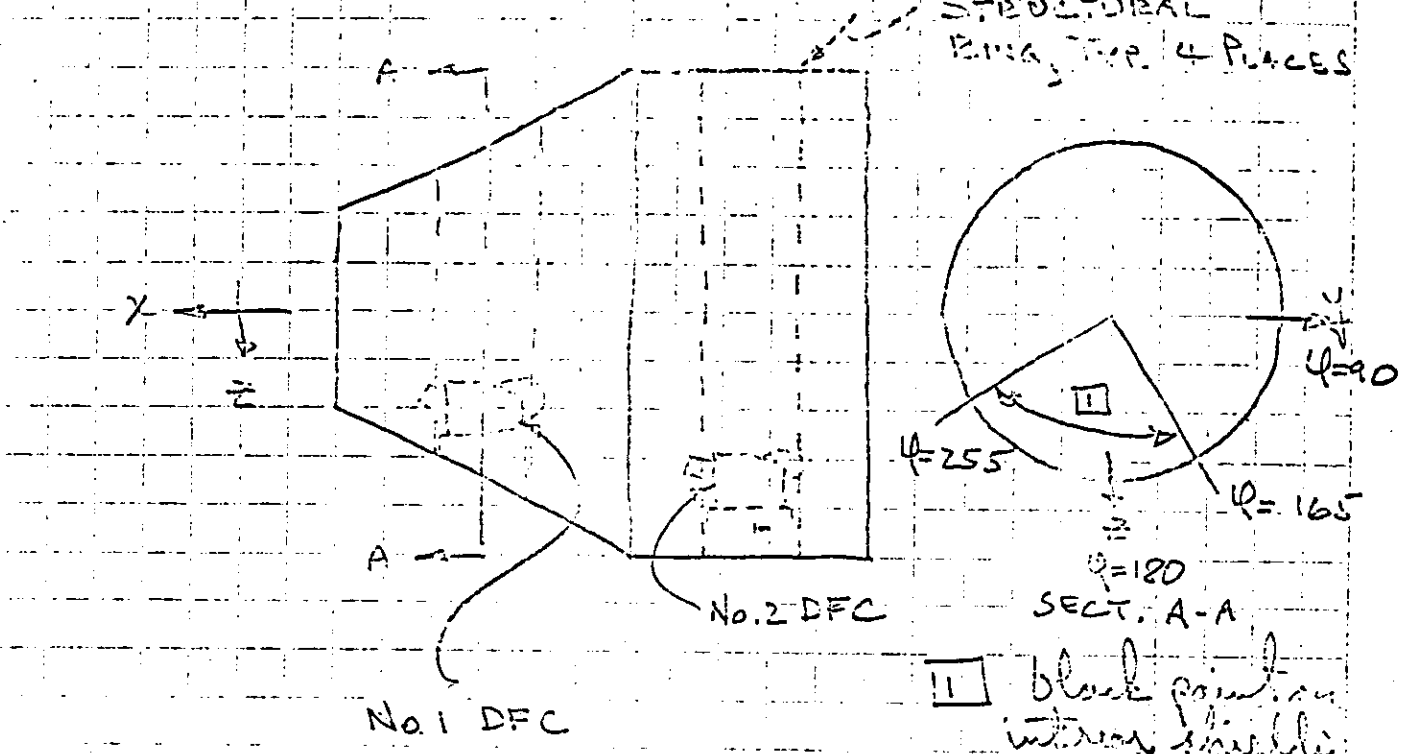

No. 1 DFC

FRONT SURFACE (FACING +X) & STELLAR SURFACE (FACING +Y) ARE TAPED WITH Al FOIL & OTHER SURFACES BLACK

No. 2 DFC

TOP SURFACE (FACING −Z) IS 50% TAPE & STELLAR SURFACE (FACING +Y) IS 100% TAPE & OTHER SURFACES BLACK

[redacted]

~~SECRET~~

[redacted]

DFC BLACK PATCHES

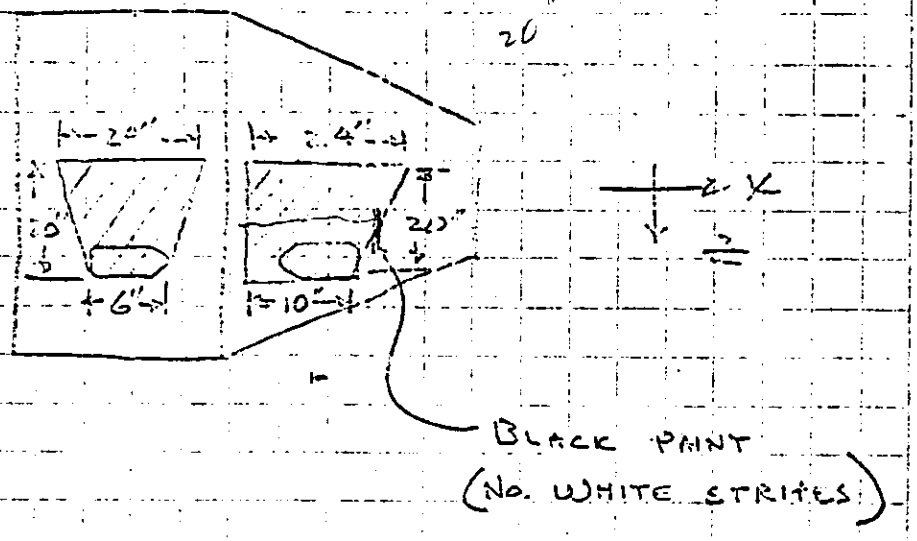

[redacted]

~~SECRET~~

[redacted]

[redacted]

[redacted]

APPENDIX B

DERIVATION OF THE SATELLITE'S ANGULAR POSITION FROM THE TERMINATOR PLANE

In Figure 1. the origin O is assumed to be at the earth's center. In addition set

E the north ecliptic pole

N a unit vector along the north equatorial pole

O a unit vector along the orbital normal

S a unit vector along the earth-sun line

P a unit vector along the earth-satellite line

T a unit vector in the direction of the ascending intersection of the orbit and terminator plane

V a unit vector in the direction of the vernal equinox

P' the projection of P onto the equatorial plane

S' the projection of S onto the equatorial plane

The following angles are assumed to be known quantities:

sun's right ascension

i orbital inclination with the equator

the angle from the north pole to the satellite position (90 minus its latitude)

Z 23-1/2°

(180 -) where is the angle between the orbital plane normal as defined by the right-hand rule and the earth-sun line. can vary from 0 to 180°

A relationship between the known quantities and the angle θ is required. The angle θ is the position of the satellite in its orbit as measured from its ascending cross of the terminator plane

$$\hat{O} \times \hat{S} \cdot \hat{O} \times \hat{P} = \begin{vmatrix} \hat{O} \cdot \hat{O} & \hat{O} \cdot \hat{P} \\ \hat{S} \cdot \hat{O} & \hat{S} \cdot \hat{P} \end{vmatrix}$$

$$\sin (180 - \beta') \cos (\theta - 180 + 90) = \cos \gamma - 0$$

$$\sin \beta' \sin \theta = \cos \gamma \qquad (1)$$

$$\hat{N} \times \hat{P} \cdot \hat{N} \times \hat{S} = \begin{vmatrix} \hat{N} \cdot \hat{N} & \hat{N} \cdot \hat{S} \\ \hat{P} \cdot \hat{N} & \hat{P} \cdot \hat{S} \end{vmatrix}$$

$$\sin \xi \sin \chi \cos (\theta - \phi) = \cos \gamma - \cos \xi \cos \chi \qquad (2)$$

$$\hat{N} \times \hat{E} \cdot \hat{N} \times \hat{S} = \begin{vmatrix} \hat{N} \cdot \hat{N} & \hat{N} \cdot \hat{S} \\ \hat{E} \cdot \hat{N} & \hat{E} \cdot \hat{S} \end{vmatrix}$$

$$\sin Z \sin \chi \cos (90 + \psi) = 0 - \cos Z \cos \chi$$

$$\tan \psi = \frac{\operatorname{ctn} Z}{\sin \psi} \qquad (3)$$

(ψ can be either 1st or 2nd quadrant)

$$\hat{N} \times \hat{O} \cdot \hat{N} \times \hat{S} = \begin{vmatrix} \hat{N} \cdot \hat{N} & \hat{N} \cdot \hat{S} \\ \hat{O} \cdot \hat{N} & \hat{O} \cdot \hat{S} \end{vmatrix}$$

$$\sin i \sin \chi \cos (\theta - 90^\circ - \phi) = \cos (180 - \beta') - \cos i \cos \chi$$

$$\cos (90 - \theta + \phi) = \frac{-\cos \beta' - \cos i \cos \chi}{\sin i \sin \chi} \qquad (4)$$

From right spherical trigonometric relationships the following equations are obtained.

$$\tan \quad = \frac{\cos Z}{\text{ctn}} \tag{5}$$

$$\csc \ 360 - (\quad - \ ) \ = -\csc(\quad - \ ) = \frac{\tan i}{\text{ctn}} \tag{6}$$

From these six relationships the value of can be computed for the given orbital data. However, there will arise ambiguous values for : instead of two values corresponding to the sun-lit side and the night side, there will be in general four solutions. It is necessary, therefore, to derive equations to test the value of for their applicability. These are derived as follows.

$$\hat{O} \times \hat{N} \cdot \hat{O} \times \hat{P} = \begin{vmatrix} \hat{O}\cdot\hat{O} & \hat{O}\cdot\hat{P} \\ \hat{N}\cdot\hat{O} & \hat{N}\cdot\hat{P} \end{vmatrix}$$

$$(\sin i)\ (1) \cos (\quad + \Delta + 90 - 180) = \cos \quad - 0$$

$$\cos \quad = \sin i \cos (\quad + \Delta - 90)$$

$$\cos \quad = \sin i \cos (90 - \quad - \ )$$

$$\cos \quad = \sin i \sin (\quad + \Delta) \tag{7}$$

Given , i, and compute Δ from the law of cosines as given in any spherical trigometry text.

$$\cos \lambda = -\cos \beta' \cos i + \sin \beta' \sin i \cos \Delta$$

$$\cos \Delta = \frac{\cos \lambda + \cos \beta' \cos i}{\sin \beta' \sin i} \qquad (8)$$

There is only one acceptable value of A, that is, $\Delta \leq 180^\circ$ since it is the angle for crossing the terminator as measured from the ascending equatorial node.

Ordinarily the value of β' is not given as such; instead a value $\beta = 90 - \beta'$ is given. This value for an afternoon launched, north-south orbit is such that the value of Ω, the angle between the orbit plane normal and the earth-sun line, is greater than 90° and $\Omega = \beta + 90^\circ$ and accordingly $\beta' = 180 - \Omega = 180 - 90 - \beta$ or $\beta' = 90 - \beta$. The orbit-plane normal in this case points away from the sun direction. For a morning launch, again north-to-south, the orbit-plane normal (right-hand rule) points toward the sun direction, the angle $\Omega < 90^\circ$ and hence $\beta' > 90^\circ$. Also, for a morning launch, again north-to-south, the angle $(\lambda - \beta - 90^\circ)$ will always be greater than 180°. For an afternoon, north-to-south launch, it will be less than 180°.

The two values obtained for $(\lambda - \zeta)$ for the sin $(\lambda - \zeta)$ are both pertinent solutions. One value corresponds to the orbital point latitude of $(90^\circ - \beta)$ for the sun-lite side and the other to the dark side of the earth. For the angular inclination, $i < 90^\circ$ the smaller value of $(\lambda - \zeta)$ corresponds to the sun-lit side while for $i > 90^\circ$ the smaller values correspond to the dark side.

SECRET

SECRET

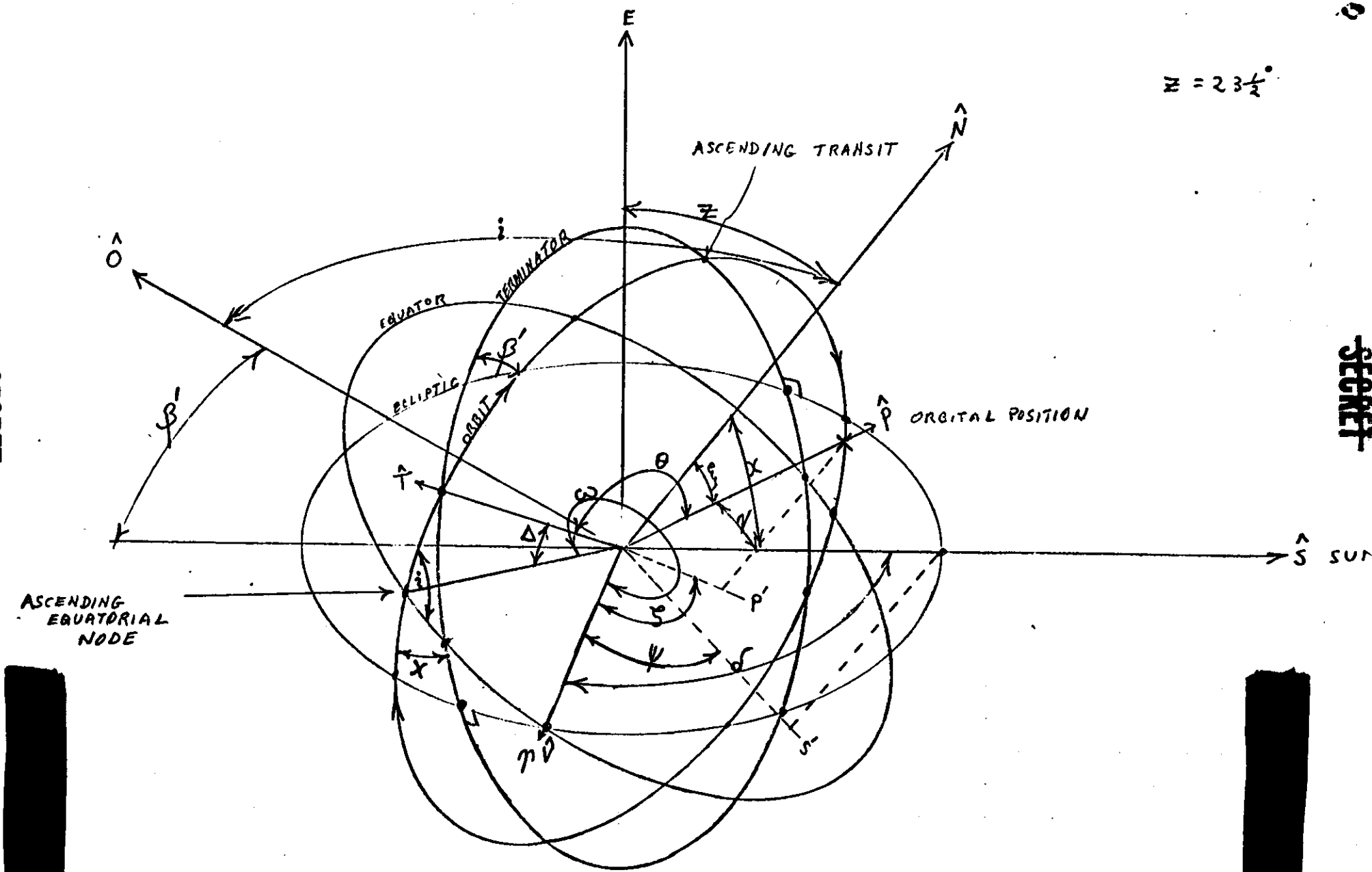

$\varepsilon = 23\frac{1}{2}°$

[redacted]

[redacted]

[redacted]

APPENDIX C

AN ESTIMATE OF THE "J" SYSTEM TEMPERATURE VARIATION TO BE EXPECTED FOR VARIATIONS OF EARTH-CLOUD COVER

An estimate of the effect of the expected cloud-cover variation upon the "J" system mean orbital temperature can be obtained by using the results of the measurements of the earth albedo by Danjon and Dubois (Ref. 5). Their measurements, made over a period of several years, indicate that the earth's albedo varies over a range of about +0.12 and -0.08 from its mean value. Their measurements were averaged in blocks of 1 month each and, hence, possibly larger variations occurred for shorter periods of time but in the averaging process they are not apparent. The assumption is made here that the magnitudes of the variations in their measurements from the mean are indicative of the magnitudes of terrestrial reflectivity variations that can be expected to exist from one "J" system flight to another.

The equation derived in Appendix E relating the system orbital mean-skin temperature to the environmental heat fluxes is

$$\overline{T^4} = \frac{\alpha}{\varepsilon} (\bar{G}_S + \bar{G}_A) + \bar{G}_e$$

The albedo flux, $\bar{G}_A$, incident on the satellite is related to the earth reflected radiation by the equation

$$\bar{G}_A = k_A \underline{a} E$$

where

k_A is a constant derived from the satellite geometry and the particular satellite orbit involved (this is apparent from the equation for the albedo flux of Appendix E.)

[redacted]

$\underline{a}$ is the terrestrial reflectivity or albedo constant

E is the solar constant

For a given satellite orbit, including its β angle[1], the variation of the value of $\bar{G}_A$ is just proportional to the variation of $\underline{a}$. The values of $\bar{G}_s$ and $\bar{G}_A$ as a function of β angle for an earth oriented cylindrical satellite at an altitude of 150 statute miles are presented in Figures 1 and 2. For a β angle of 40° and for $\underline{a}$ = 0.39

$$\bar{G}_A = 16.4 \text{ Btu/hr-ft}^2$$

$$\bar{G}_s = 69.3 \text{ Btu/hr-ft}^2$$

The use of the earthshine equation of Appendix F and the use of the equivalent earth black body temperature of 452° R results in

$$\bar{G}_e = 28.4 \text{ Btu/hr-ft}^2$$

The "J-7" system designed paint mosaic for the cylindrical barrel had an α/ϵ = 1.086. The mean orbital skin temperature computed by the above equation results in

$$\left[\overline{T^4}\right]^{\frac{1}{4}} = 516^\circ \text{ R} \quad \text{or} \quad 56^\circ \text{ F}$$

The increase of $\underline{a}$ by +0.12 in accordance with the positive variation found by Danjon and Dubois results in a value of G'_A of $G'_A = (\frac{0.51}{0.39})\ (16.4) = 21.6 \text{ Btu/hr-ft}^2$ for which the use of the above equation results in

$$\left[\overline{T^4}\right]^{\frac{1}{4}} = 522^\circ \text{ R} \quad \text{or} \quad 62^\circ \text{ F}$$

This is an increase of 6° F in the mean temperature.

---

[1]The orbital β angle is the angle subtended by the orbital plane with the earth-sun line.

For the negative variation of -0.08 found by Danjon and Dubois in their measurements of the albedo constant similar computations to those above result in a value of

$$\left[\overline{T^4}\right]^{1/4} = 512^\circ \text{ R} \quad \text{or} \quad 52^\circ \text{ F}$$

This is a decrease by 4° F.

For the above computations the assumption is made that the earthshine flux remains constant during the terrestrial reflectivity, or albedo constant, fluxuations. Since the earthshine is the solar energy initially absorbed by the earth and then reradiated back to space the energy balance requires that the absorbed solar energy is proportional to $(1 - \bar{a})$ where $\bar{a}$ is the mean terrestrial reflectivity, or albedo constant. For a steady-state condition this is true; however, for short time period variations of $\bar{a}$ (a few days) the thermal inertial mass of the earth is such that the earthshine flux is relatively constant. Albrecht computes a heat reservoir of about 1.6×10^5 Btu/hr per square foot of the earth's surface (Ref. 6, p. 2-2). Lettau and Haugen in the same reference, p. 2-1, state that 100 days of radiation from the earth would be required to deplete this reservoir if all energy inputs to the earth were to cease. Thus, the assumption of a constant earthshine flux for a period of a few days during a change in the albedo constant of +0.12 or -0.08 appears to be valid.

For the assumption that the magnitude of the monthly variation in the earth albedo constant as measured by Danjon

and Dubois represent the variations that might be expected to occur over short intervals of time, the resulting mean orbital temperature variation to be expected for the "J" system satellite from this source alone, is approximately its mean temperature $+6^{\circ}$, -4° F.

MEAN SOLAR FLUX TO A HORIZONTAL, CYLINDRICAL SURFACE AVERAGED OVER THE CYLINDRICAL SIDES AND OVER ALL ORIENTATIONS FOR A CIRCULAR, POLAR ORBIT FLYING AT ALTITUDE OF 150 N. MI.
THE SOLAR CONSTANT = 443 BTU/HR-FT²

MEAN SOLAR FLUX AVERAGED OVER ORBIT, BTU/HR-FT²

440
430
420
410
400
390
380
370
360

0 10 20 30 40 50 60 70 80 90

ORBIT INCLINATION (DEGREES)

(RETROGRADE ORBITS ARE NOT INCLUDED)

[redacted]

APPENDIX D

THE EFFECT OF THE MEAN TERRESTRIAL REFLECTIVITY UPON THE ORBITAL MEAN TEMPERATURE LEVEL OF AN EARTH ORBITING SATELLITE

The earthshine flux, G_e, to a satellite is directly proportional to the earth's emissive power, σT_e^4, (Appendix E) where T_e is the black-body temperature of the earth and σ is the Stephan-Boltzman radiation constant. This can be expressed mathematically as

$$G_e = k_e \left(\sigma T_e^4\right)$$

where k_e is a constant of the geometry and particular satellite orbit. For an equilibrium or steady-state condition the solar energy absorbed by the earth is reradiated to space; this is expressed by

$$(4\pi R^2) \left(\sigma T_e^4\right) = (\pi R^2)(E)(1 - a)$$

where

- R earth's radius
- E solar constant
- a the mean terrestrial reflectivity (for this case, the entire earth, it is the planetary albedo)

The left-hand side of the above equation is the total energy radiated to space; the right-hand side is the total solar energy absorbed by the earth. Accordingly, the earth's emissive power, σT_e^4, is

$$\sigma T_e^4 = \frac{E(1 - a)}{4}$$

[redacted]

SECRET

Thus,

$$G_e = (k_e)\left[\frac{E(1 - a)}{4}\right]$$

The albedo flux, G_A, to a satellite is directly proportional to the solar energy reflected from the earth's surface (Appendix E). Mathematically, this is expressed as

$$G_A = k_A a E$$

where k_A is a constant similar to k_e. The value of a for the albedo flux is more dependent upon the local portion of the earth's surface viewed by the satellite than is the a for the earth's emissive power above. However, their values for polar orbits are close numerically and will be assumed to be equal for this analysis.

From Appendix E the equation for the orbital mean temperature of a satellite is

$$\sigma T^4 = G_e + \frac{\alpha_A}{\epsilon} G_A + \frac{\alpha_S}{\epsilon} G_S$$

It is assumed that the emissivity, ϵ, is for the range of values encountered for T equal to the absorptivity value. By assuming that $\alpha_A \approx \alpha_S$,

$$\sigma T^4 = G_e + \left(\frac{\alpha}{\epsilon}\right) G_A + \left(\frac{\alpha}{\epsilon}\right) G_S$$

Upon substitution of the above expressions for G_e and G_A the equation becomes

$$\sigma T^4 = k_e\left[\frac{E(1 - a)}{4}\right] + \left(\frac{\alpha}{\epsilon}\right) k_A a E + \left(\frac{\alpha}{\epsilon}\right) G_S$$

Allowing the constants k_e and k_A to absorb the constants $E/4$ and $(\alpha/\epsilon)E$ the equation further reduces to

$$\sigma T^4 = k'_e(1 - a) + k'_A a + \left(\frac{\alpha}{\epsilon}\right) G_S$$

Partially differentiating with respect to a results in

$$\frac{\partial(\sigma T^4)}{\partial a} = - k_e + k_A$$

which for $k'_e = k'_A$ vanishes.

The value of k'_e, defined as $k_e E/4$, is

$$k'_e = \frac{G_e}{1 - a}$$

For a value of a of 0.39 the value of G_e for the earthshine equation of Appendix F is $G_e = 26.2$ Btu/hr-ft^2 and

$$k'_e = \frac{26.2}{0.61} = 43.0 \text{ Btu/hr-ft}^2$$

where k'_e is a constant of the satellite and orbit geometry and is independent of the value of a used. The value of G_e varies directly as $(1 - a)$.

The value of k'_A with the absorbed $(\alpha/\epsilon)(E)$ is

$$k'_A = \left(\frac{\alpha}{\epsilon}\right)\left(\frac{G_A}{a}\right)$$

which, for $\beta = 40^\circ$ and $a = 0.39$, $G_A = 16.4$ Btu/hr-ft^2 (Appendix C, Fig. C.2). And, for $\alpha/\epsilon = 1.086$,

$$k'_A = (1.086)\left(\frac{16.4}{3.9}\right) = 45.7 \text{ Btu/hr-ft}^2$$

and, thus,

$$\frac{\partial(\sigma\overline{T^4})}{\partial a} = + 2.7 \text{ Btu/hr-ft}^2$$

The value of $\sigma\overline{T^4}$ at $\beta = 40^\circ$ is 26.2 Btu/hr-ft^2 for the above assumed value of $a = 0.39$; and for $G_S = 69.3$ Btu/hr-ft^2 from Appendix C, Figure C.1, and $\alpha/\epsilon = 1.086$ for the present example.

$$\sigma\overline{T^4} = 26.2 + (1.086)(16.4 + 69.3)$$

$$= 119.2 \text{ Btu/hr-ft}^2$$

$$\left[\overline{T^4}\right]^{1/4} = 514^\circ \text{ R}$$

Replacing the differentials by finite increment symbols,[1]

$$\frac{\partial(\sigma\overline{T^4})}{\partial a} = \frac{\Delta(\sigma\overline{T^4})}{\Delta a} = + 2.7 \text{ Btu/hr-ft}^2$$

Values for a given in the literature range from 0.34 to 0.43 (Ref. 8, p. 166). Hence, an assumption that $\Delta a \approx \pm 0.1$ is quite conservative, and, accordingly

$$\Delta(\sigma\overline{T^4}) \approx \pm 0.27 \text{ Btu/hr-ft}^2$$

For the above value of $\sigma\overline{T^4} = 119.2$ Btu/hr-ft^2, the value of

$$\Delta\left[\overline{T^4}\right]^{1/4} \ll 1^\circ \text{ F}$$

---

[1]This is correct mathematically for this case since σT^4 varies linearly as a function a.

and, hence, the orbital mean temperature of the system is effectively independent of the mean or long-term terrestrial reflectivity. This is the reflectivity as averaged over a period of several weeks.

[redacted]

APPENDIX E

SATELLITE, ORBITAL MEAN TEMPERATURE COMPUTATIONS

The rate of change of the space averaged skin temperature of a satellite space vehicle, such as the "J" system, is

$$m\,c\,\frac{dT}{d\theta} = \alpha_s\,G_s + \alpha_A\,G_A + \epsilon\,G_e - \epsilon\sigma T^4 \qquad (1)$$

where

m	unit area skin mass
c	specific heat of the material
G_s	direct solar heat fluxes averaged over the skin
G_A	albedo heat fluxes averaged over the skin
G_e	earthshine heat fluxes averaged over the skin
θ	time
α_s	solar energy absorptivitive
α_A	albedo energy absorptivitie
ϵ	emissivity

The emissivity, ϵ, is applicable for both the absorptivity for the earthshine and the emissivity of the vehicle skin since ϵ for the paint materials and the gold surface finish of the "J" system as a function of temperature changes very little over the range of the earth's effective temperature, 454° R, and the maximum skin temperature, about 700° R. This is evident from the curves of reflectivity for these materials presented in Reference 7.

The rate of change of G_s and G_A with the orbit precession, about $2\frac{1}{2}^{\circ}$ per day, is such that the mean skin

[redacted]

temperature averaged over one orbital revolution changes but slightly from one orbital revolution to the succeeding one. There are about 16 orbital revolutions per day such that the orbital β angles for two successive revolutions differ by less than 0.2°. From the curves of G_s and G_A as a function of β angle, Appendix C, Figures 1 and 2, this is seen to result in a change of G_s and G_A at β angle = 53° of less than two-tenths of one percent; this is considered negligible since the temperature varies as the fourth root of the heat flux; a 0.2 percent variation in the heat flux at a 530° R mean temperature would cause a temperature variation of about 0.2° R. The "J" systems have a magnesium skin of approximately 0.070-inch thick. The time constant for the skin having $\alpha/\epsilon \approx 1$ is about 8 minutes, Appendix G. Since the orbital period is more than ten times[1] this, the orbital mean temperature of the vehicle skin will be very nearly the mean equilibrium temperature corresponding to that orbit's mean thermal environment. Thus, the integration with time of Equation (1) over an orbital period will result in a mathematical relationship between the vehicle skin mean temperature and the mean thermal environment that is applicable to any one single orbital revolution chosen from a succession of such revolutions. The resulting equation is, since

$$\int_{\text{period}} dT/d\theta = \text{zero}$$

$$\epsilon \overline{T^4} = \alpha_s \overline{G_s} + \alpha_A \overline{G_A} + \epsilon \overline{G_e} \qquad (2)$$

[1]The orbital period for the "J" system is about 90 minutes, Appendix A.

In general, where α_s, α_A, and ϵ vary over the vehicle surface, it is necessary to perform the time and space averaging as indicated by the bars in Equation (2); in the present case, however, the vehicle skin paint pattern is designed to provide a constant α_s, α_A, and ϵ as a function of position around the body; this is true to within the dimensions of the paint pattern stripping width of a few inches. Thus, the α and ϵ values can be separated from the terms $\overline{T^4}$, $\overline{G}_s$, and $\overline{G}_e$; and for the assumption that $\alpha_s \approx \alpha_A$, this results in the equation

$$c\,\overline{T^4} = (\overline{\alpha}/\overline{\epsilon})\ (\overline{G}_s + \overline{G}_A) + \overline{G}_e \qquad (3)$$

The values of $\overline{\alpha}$ and $\overline{\epsilon}$ depend upon the relative area proportions covered by the various surface finishes making up the thermal control surface mosaic of the skin. For the present systems two surface finishes are used, white paint and gold. Let x be the proportion of the skin area covered by the paint having an absorptivity, α_p, and an emissivity, ϵ_p, and (1-x) be that proportion covered by gold having α_g and ϵ_g. Then

$$\frac{\overline{\alpha}}{\overline{\epsilon}} = \frac{x\,\alpha_p + (1 - x)\,\alpha_g}{x\,\epsilon_p + (1 - x)\,\epsilon_g} \qquad (4)$$

and upon solving for x,

$$x = \frac{\epsilon_g - \left(\frac{\overline{\epsilon}}{\overline{\alpha}}\right)\alpha_g}{\left(\frac{\overline{\epsilon}}{\overline{\alpha}}\right)\left(\alpha_p - \alpha_g\right) + \left(\epsilon_g - \epsilon_p\right)} \qquad (5)$$

For any desired $\bar{\alpha}/\bar{\epsilon}$ Equation (5) can be used to compute the percent of paint ($x \times 100$) necessary for its composition. The individual values of $\bar{\alpha}$ and $\bar{\epsilon}$ can be obtained then from the numerator and the denominator respectively of Equation (4).

[redacted]

APPENDIX F

THERMAL RADIATION FLUX TO A SATELLITE

This Appendix consists of a number of Appendices originally compiled for Vidya Report No. 51. It is a self-contained unit; all references made therein pertain to sections internal to Appendix F.

[redacted]

[redacted]

APPENDIX A'

SYMBOLS USED IN APPENDICES B', C', AND D'

A	area of orbiting surface
E	solar constant, 443 Btu/hr-ft^2
F	radiation flux, Btu/hr-ft^2
T	absolute temperature, ^{o}R
a	albedo of earth, average ≈ 0.35
dS	area element of earth's surface
h	satellite altitude
k	absorption coefficient
r_o	mean radius of earth, 3960 statute miles
x,y,z	orthogonal coordinates
α	angle made by the normal to the earth's surface element with the line connecting that element to the orbiting surface
β	angle made by the normal to the insolated earth surface element with the line connecting that element to the sun
δ	angle made by the x-y plane projection of the normal to the irradiated surface with the orbit path of the satellite
ϵ	surface emissivity
ζ	angle in the x-y plane made by the plane of the orbit to the y axis
η	angle made by the normal to the orbiting surface with the line connecting it to the earth surface element
θ_s	angle made by the sun to earth line with the z axis
θ,ϕ	spherical coordinate angles

[redacted]

λ	Angle made by the line of apsides with the earth-sun line. For a circular orbit, the angle made made by the earth-sun line with the orbit planes
ξ	angle of orbiting surface normal to z axis
ρ	the distance between the earth surface element and the orbiting surface
σ	Stephen-Boltzmann constant
χ	angle subtended in the x-y plane by the irradiated surface normal and the y axis
ψ	angle made by the line of apsides with the z axis
Ω	angle made by the normal to the orbit plane with the earth-sun line

[redacted]

APPENDIX B

HEAT FLUX DUE TO THE SUN'S REFLECTION FROM THE EARTH

Basic Equation

The radiant energy from the sun is partially absorbed and partially reflected from the earth's surface. The reflected energy from any earth surface element, dS, produces a radiant heat flux on a satellite which is in view of the reflecting surface element.

The basic equation for energy reflecting from an earth surface element, dS, and striking the satellite surface element, dA, is

$$dq = aE \frac{\cos \alpha \cos \beta \cos \ddot{\eta} \, dA \, dS}{\pi \rho^2}$$

Symbols are defined in Appendix A.

The satellite coordinates in space with respect to the sun and to the earth's surface must be designated. Also, for a given satellite-earth-sun geometry the orientation of the satellite surface point of interest (for heat flux calculation) must be designated.

The position of the satellite will be designated by the orientation of the orbit plane in space relative to the sun, the eccentricity of the orbit, and orbit perigee.

The surface orientation is designated by the relationship of the satellite surface normal angles made in the coordinate system to the earth's surface and to the sun in the same coordinate system.

The position of the satellite determines the coordinate system orientation with respect to the satellite-earth-sun system. The earth's center is the origin of the coordinate system; the satellite is always on the z axis. The y-z plane is established as the plane containing the satellite, earth, and sun.

In Figure B.1 it is seen that the angles Ω, λ, and ψ determine the satellite position relative to the earth and the sun. For a satellite time in orbit of approximately 4 days, the variation of the orbit position due to precession or perigee tumbling is assumed negligible. Thus Ω and λ will be orbit constants and ψ is the positioning variable.

The variables ϕ and θ establish the position of any earth surface element.

[redacted]

The term $\cos \alpha$ is derived from Figure B'.2

$$\rho = \frac{\sin \theta}{\sin \alpha} (h + r_o)$$

and

$$\frac{r_o \sin \alpha}{h + r_o} = \sin(\alpha - \theta) = \sin \alpha \cos \theta - \cos \alpha \sin \theta$$

$$\sin \alpha \left[\cos \theta - \frac{1}{1 + (h/r_o)}\right] = \cos \alpha \sin \theta$$

so

$$\tan \alpha = \frac{\left[1 + (h/r_o)\right] \sin \theta}{\left[1 + (h/r_o)\right] \cos \theta - 1}$$

setting

$$y = h/r_o$$

$$\cos \alpha = \frac{(1 + y)\cos \theta - 1}{\left[(1 + y)^2 - 2(1 + y)\cos \theta + 1\right]^{1/2}}$$

The term $\cos \beta$ is also derived from Figure B'.2. In Figure B'.2, let (at the earthcenter)

$\vec{z}$ = a unit vector along the z axis

$\vec{S}$ = a unit vector pointing toward the sun

$\vec{r}_o$ = a unit vector pointing to the surface element of earth, dS

$$(\vec{z} \times \vec{r}_o) \cdot (\vec{z} \times \vec{S}) = \begin{vmatrix} \vec{z} \cdot \vec{z} & \vec{z} \cdot \vec{S} \\ \vec{r}_o \cdot \vec{z} & \vec{r}_o \cdot \vec{S} \end{vmatrix}$$

$$\sin \theta \cos \phi \sin \theta_S = \cos \beta - \cos \theta \cos \theta_S$$

hence

$$\cos \beta = \sin \theta \sin \theta_S \cos \phi + \cos \theta \cos \theta_S$$

The term $\cos \eta$ is also derived from the same figure. In Figure B.2, let (at the orbiting surface, dA)

$\vec{z}$ = a unit vector along the z axis

$\vec{n}$ = a unit vector along the normal to the back of the orbiting surface

$\vec{c}$ = a unit vector lying along ρ pointing toward element dS

$$(\vec{z} \times \vec{n}) \cdot (\vec{z} \times \vec{c}) = \begin{vmatrix} \vec{z} \cdot \vec{z} & \vec{z} \cdot \vec{c} \\ \vec{n} \cdot \vec{z} & \vec{n} \cdot \vec{c} \end{vmatrix}$$

$$\sin \xi \cos \left[(\pi/2 - \phi) - (\pi/2 + \chi)\right] \sin \gamma = \cos(\pi - \eta) - \cos \xi \cos \gamma$$

and

$$\gamma = \pi - (\alpha - \theta) = (\pi + \theta) - \alpha$$

From the law of sines is derived

$$\tan \alpha = \frac{(1 + y)\sin \theta}{(1 + y)\cos \theta - 1}$$

so

$$\gamma = \pi + \theta - \tan^{-1}\left[\frac{(1 + y)\sin \theta}{(1 + y)\cos \theta - 1}\right]$$

and

$$\sin \gamma = \sin(\pi + \theta)\cos\left\{\tan^{-1}\left[\frac{(1 + y)\sin \theta}{(1 + y)\cos \theta - 1}\right]\right\} - \cos(\pi + \theta)\sin\left\{\tan^{-1}\left[\frac{(1 + y)\sin \theta}{(1 + y)\cos \theta - 1}\right]\right\}$$

$$\sin \gamma = \frac{\sin \theta}{\sqrt{(1 + y)^2 - 2(1 + y)\cos \theta + 1}}$$

$$\cos \gamma = - \frac{(1 + y) - \cos \theta}{\sqrt{(1 + y)^2 - 2(1 + y)\cos \theta + 1}}$$

Now

$$\cos(\pi - \eta) = - \cos \eta = - \sin \gamma \sin \xi \cos(\phi - \chi) + \cos \gamma \cos \xi$$

so

$$\cos \eta = \frac{\left[(1 + y) - \cos \theta\right] \cos \xi + \sin \theta \sin \xi \cos(\phi - \chi)}{\left[(1 + y)^2 - 2(1 + y)\cos \theta + 1\right]^{1/2}}$$

For

$$dS = r_o^2 \sin \theta \, d\phi \, d\theta$$

the equation to be integrated is

$$\frac{\pi F_{S-A}}{aE} = \int^{\theta} \int^{\phi} \frac{\sin \theta}{\left[(1 + y)^2 - 2(1 + y)\cos \theta + 1\right]^2} \Big((\sin \theta \sin \theta_S \cos \phi + \cos \theta \cos \theta_S) \left[(1 + y)\cos \theta - 1\right] \Big\{ \left[(1 + y) - \cos \theta\right] \cos \xi + \sin \theta \sin \xi \cos(\phi - \chi) \Big\} \Big) \, d\phi \, d\theta$$

Circular Orbits

For a noon-launched, circular, polar orbit, y is a constant and the angle χ is just a function of the satellite surface point orientation with respect to the orbit path. The y axis in this case is tangent to the orbit path.

The equation is readily integrated with respect to the variable ϕ.

$$\frac{\pi F_{S-A}}{aE} = \int^{\theta} \frac{[(1+y)\cos\theta - 1]\sin\theta}{[(1+y)^2 - 2(1+y)\cos\theta + 1]^2} \Big(\sin\theta \sin\theta_S \sin(\phi) \cos\xi \left[(1+y) - \cos\theta\right] + \sin^2\theta \sin\theta_S \sin\xi \left\{ \left[\frac{\phi}{2} + \frac{\sin 2(\phi)}{4}\right] \cos\chi + \frac{1}{2}\sin^2\phi \sin\chi \right\} + \phi \left[(1+y) - \cos\theta\right] \cos\theta \cos\theta_S \cos\xi + \cos\theta \cos\theta_S \sin\theta \sin\xi \sin(\phi - \chi) \Big)^{\phi(\theta)} d\theta$$

Integration with respect to θ requires, in general, numerical methods.

For circular orbits the angle θ_S is a measure of satellite position and it is convenient to integrate numerically the equation for various values of θ_S.

For other than a noon launching the angle χ is not constant but is dependent upon position. It is then necessary to divide the angle χ into two parts. Looking downward from a position above the satellite the following sketch is applicable:

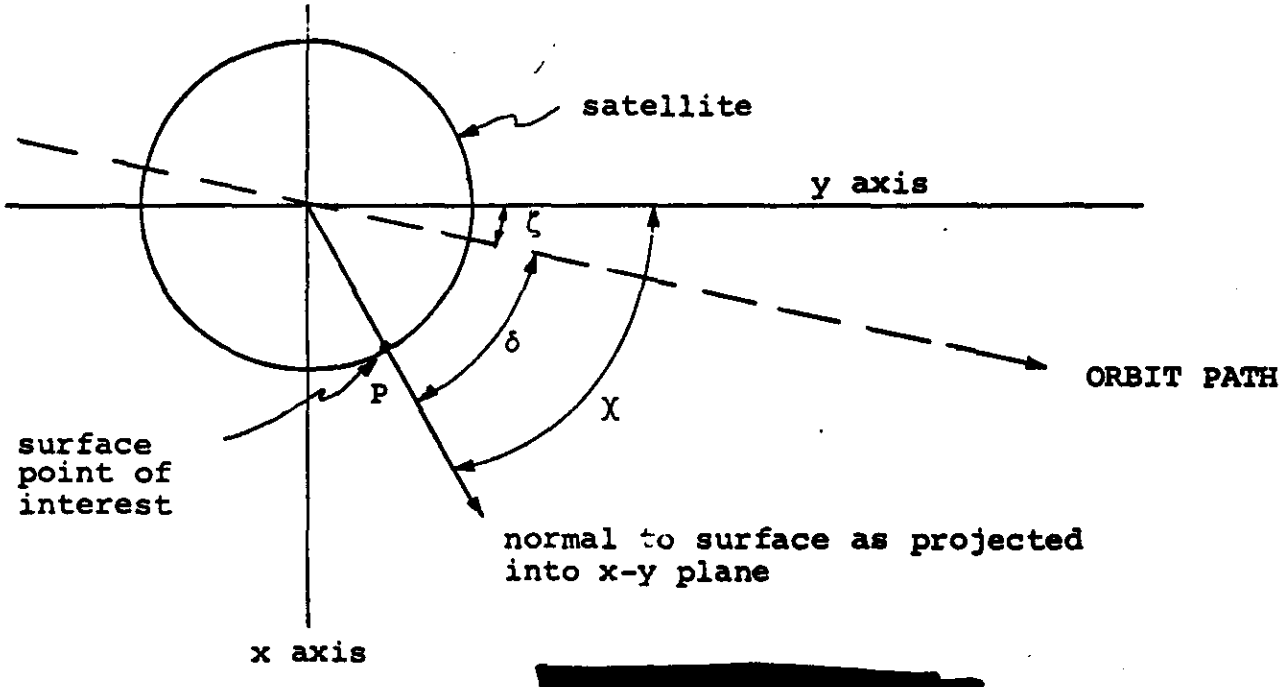

[redacted]

In the equation for the reflected flux to the point P the angle χ is found in the expression $\cos(\phi - \chi)$ for χ measured in the same direction as ϕ.

Since

$$\chi = \zeta + \delta$$

then

$$\cos(\phi - \chi) = \cos(\phi - \zeta - \delta)$$

For any one satellite surface point the angle δ is a constant (for self-orienting satellites) and ζ is a function of the orbit constants and the satellite position in the orbit.

By inspection of Figure B'.1 it is seen that

$$\sin \zeta = \frac{\cos \Omega}{\sin \theta_S}$$

This expression also shows the limiting values of the angle θ_S for an off noon launching.

Elliptic Orbits

For an elliptic orbit having the orbit constants e, λ, and Ω the value of ζ is found as follows:

In Figure B'.1, let

$\vec{z}$ = a unit vector lying along axis z

$\vec{c}$ = a unit vector lying along the line connecting the earth center with the sun center

$\vec{p}$ = a unit vector lying along the line of apsides pointing toward perigee

then

$$(\vec{z} \times \vec{c}) \cdot (\vec{z} \times \vec{p}) = \begin{vmatrix} \vec{z} \cdot \vec{z} & \vec{z} \cdot \vec{p} \\ \vec{c} \cdot \vec{z} & \vec{c} \cdot \vec{p} \end{vmatrix}$$

[redacted]

$$\sin \theta_S \sin \psi \cos \zeta = \cos \lambda - \cos \theta_S \cos \psi$$

$$\cos \zeta = \frac{\cos \lambda - \cos \theta_S \cos \psi}{\sin \theta_S \sin \psi}$$

This expression is set equal to

$$\cos \zeta = \sqrt{1 - \sin^2 \zeta} = \sqrt{1 - \frac{\cos^2 \Omega}{\sin^2 \theta_S}}$$

and solved for $\cos \theta_S$.

$$\cos \theta_S = \cos \psi \cos \lambda - \sin \psi \sqrt{\sin^2 \Omega - \cos^2 \lambda}$$

In computing the heat flux it is convenient to obtain θ_S with the above equation from the required position, ψ, and the orbit constants λ and Ω. The value of $\sin \theta_S$ and $\cos \theta_S$ may then be used in the flux equation. For machine computation the above expression used to obtain $\sin \theta_S$ from

$$\sqrt{1 - \cos^2 \theta_S}$$

does not distinguish among the quadrants and is therefore difficult to program.

The variation of satellite altitude for an elliptic orbit requires that y be a variable.

$$y = h/r_o$$

The equation for the radius vector of an ellipse is

$$r = \frac{a(1 - e^2)}{1 + e \cos \psi}$$

The altitude of the satellite is

$$h = r - r_o = \frac{a(1 - e^2)}{1 + e \cos \psi} - r_o$$

and

$$y = \frac{h}{r_o} = \frac{a(1 - e^2) - r_o}{r_o(1 + e \cos \psi)}$$

and

$$(1 + y) = 1 + \frac{h}{r_o} = \frac{a(1 - e^2)}{r_o(1 + e \cos \psi)}$$

Substitution of this expression into the flux equation for $(1 + y)$ extends the equation to elliptic orbits for the assumed conditions.

Integration Limits of ϕ

The variable ϕ is completely independent of the variable θ for only that portion of the earth's surface symmetrical about the z axis which may be free from the effects of shielding or of sun shadow.

If the tangent plane to a point on the curved surface of a satellite passes through the earth then all points on the earth surface to the back side of the plane are shielded from the view from that point. Radiant energy reflected from the earth from surface points to the rear of such a tangent plane will not fall on that satellite surface point. The line of demarcation on the earth surface is that for which the angle $\eta = 90^\circ$ (Fig. B.2).

Thus these limits of ϕ can be obtained by setting the expression for $\cos \eta = 0$. This results in such limits being

$$\phi = \zeta + \delta \pm \left(\cos^{-1} \left\{ \frac{\left[(1 + y) - \cos \theta\right] \operatorname{ctn} \xi}{\sin \theta} \right\} - \pi \right)$$

The sun shadow line on the earth's surface is the daylight-dark line. The ϕ limits for this line are obtained by setting the expression

$$\cos \beta = 0$$

This results in the limits

$$\phi = \pm \left[\pi - \cos^{-1} (\operatorname{ctn} \theta \operatorname{ctn} \theta_S) \right]$$

Integration Limits of θ

The limits required for the angle θ are those for the intersection of the sun shadow with the y-z plane great circle on the earth's surface, the minimum value of θ for the line of the tangent plane to the satellite surface point intersection with the earth surface, and the limit of the earth surface visible from the satellite (i.e., the horizon).

The point of intersection of the sun shadow with the y-z plane great circle of the earth is

$$\theta = \pi/2 - \theta_S$$

The point of the minimum value of θ for the tangent plane intersection with the earth surface is obtained by equating the limits of ϕ pertaining to the line of intersection of the tangent plane with the earth surface.

$$\phi = \zeta + \delta \pm \left(\cos^{-1} \left\{ \frac{\left[(1 + y) - \cos \theta \right] \operatorname{ctn} \xi}{\sin \theta} \right\} - \pi \right)$$

thus

$$\zeta + \delta + \left(\cos^{-1} \left\{ \frac{\left[(1 + y) - \cos \theta \right] \operatorname{ctn} \xi}{\sin \theta} \right\} - \pi \right)$$

$$= \zeta + \delta - \left(\cos^{-1} \left\{ \frac{\left[(1 + y) - \cos \theta \right] \operatorname{ctn} \xi}{\sin \theta} \right\} - \pi \right)$$

and

$$\theta = \cos^{-1} \left[\frac{(1 + y) \operatorname{ctn}^2 \xi \pm \sqrt{1 - y \operatorname{ctn}^2 \xi (2 + y)}}{1 + \operatorname{ctn}^2 \xi} \right]$$

The limit of θ for the earth horizon is

$$\theta = \cos^{-1} \left(\frac{1}{1 + y} \right)$$

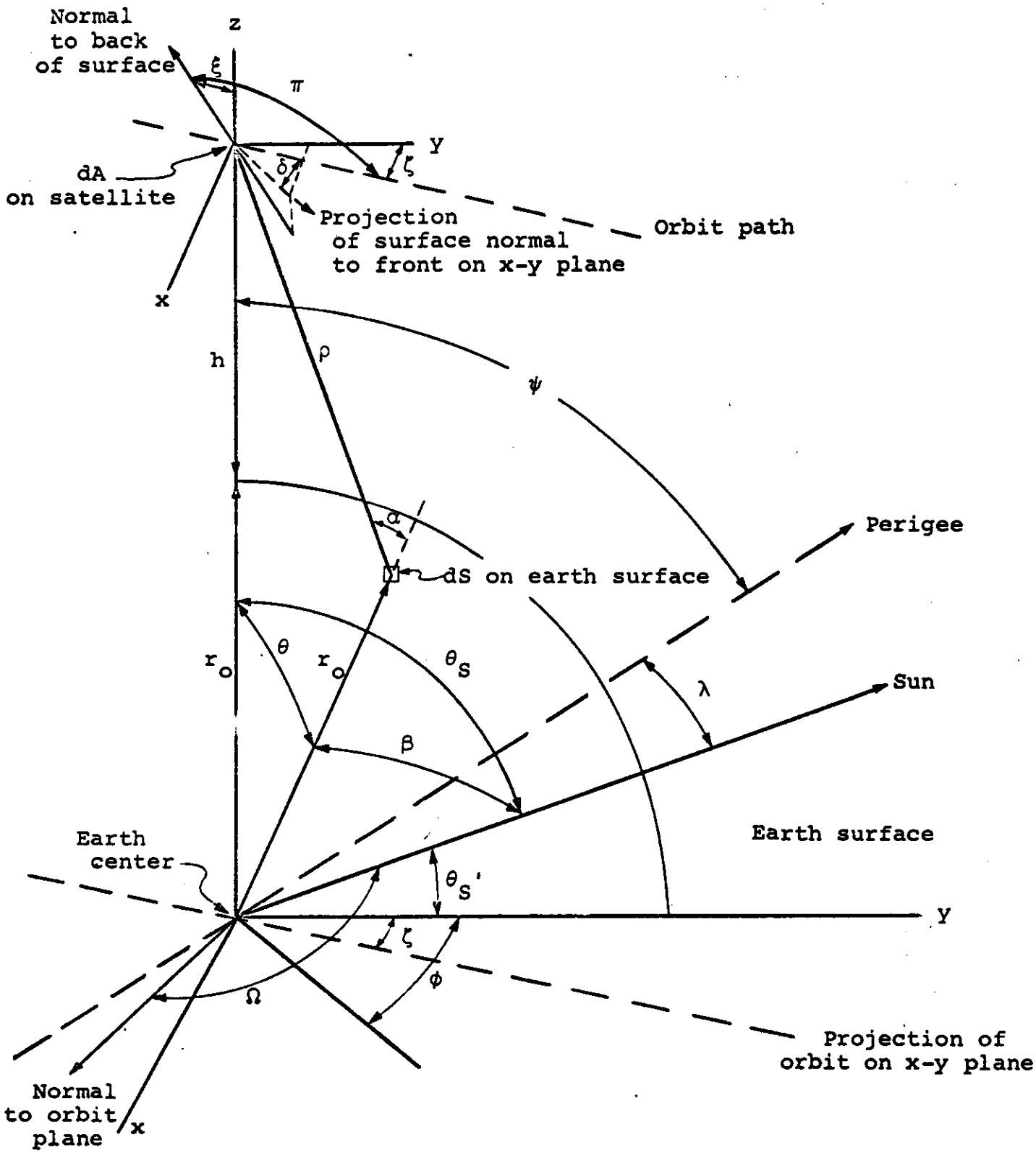

Figure B-1.- Satellite-earth-sun coordinate system.

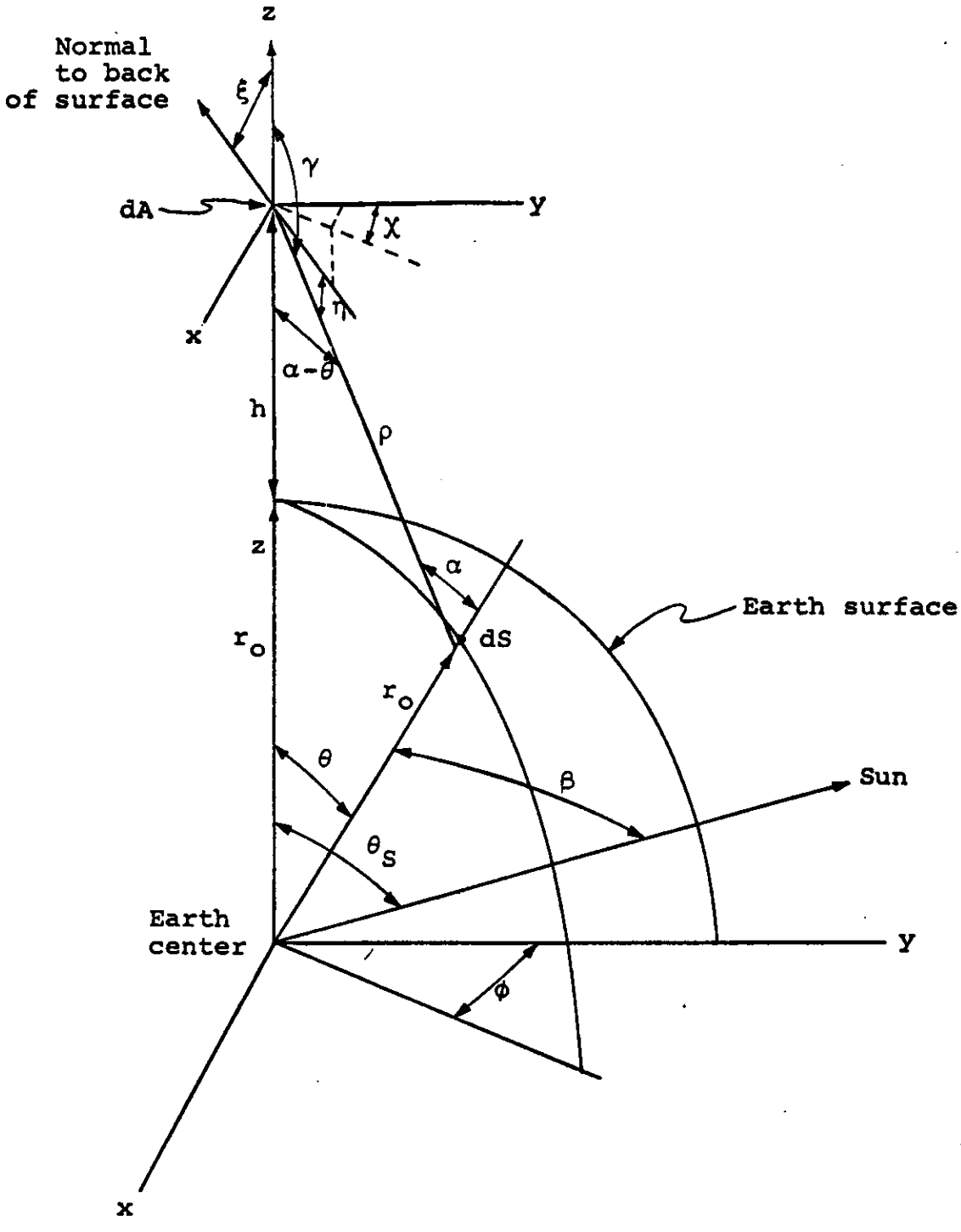

Figure B-2.- Earth-orbiting surface geometry.

[redacted]

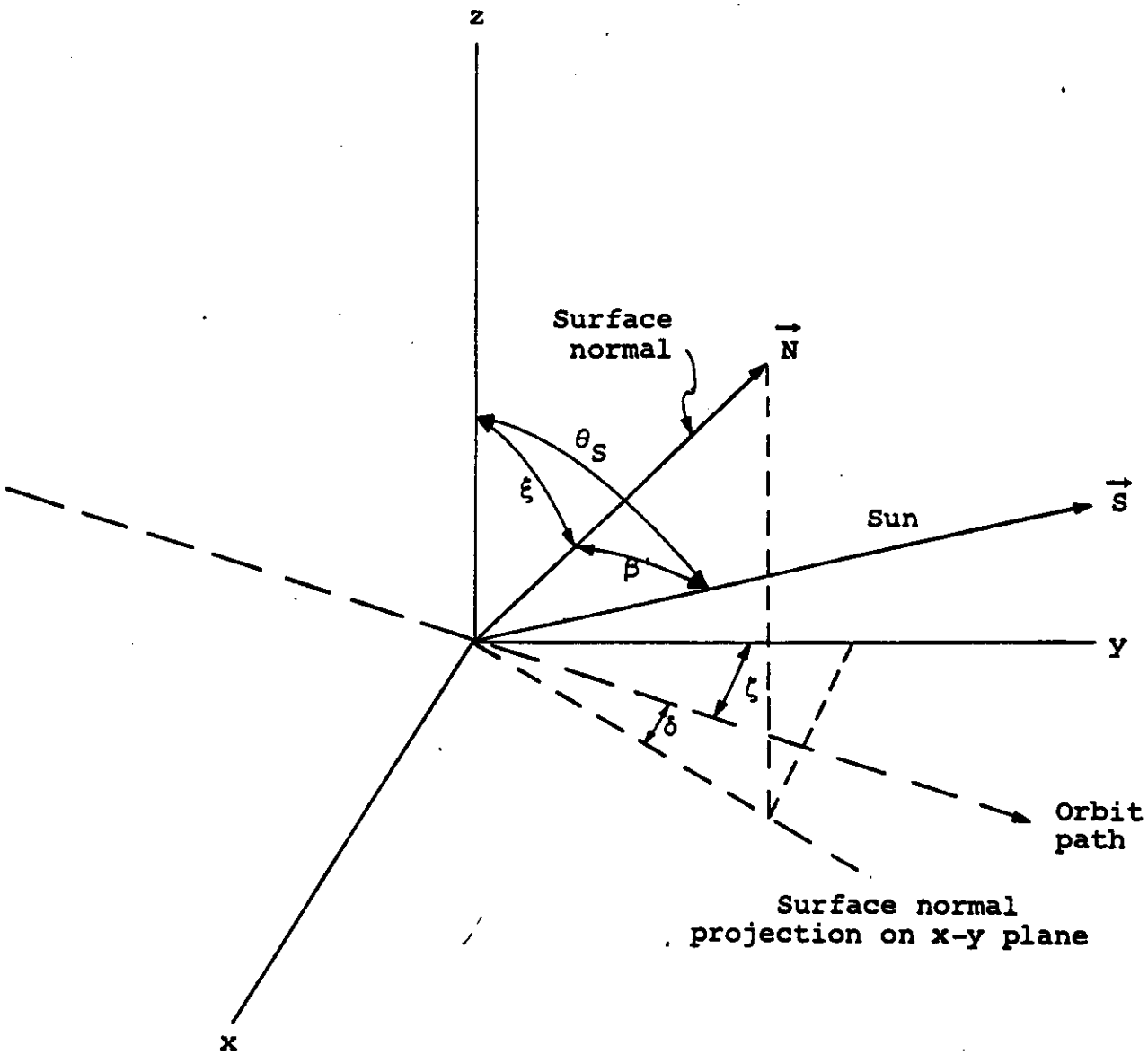

Figure B-3.- Direct insolation geometry.

[redacted]

APPENDIX C

HEAT FLUX TO A SATELLITE SURFACE DUE TO EARTH RADIATION

If the net heat transfer to the earth is zero, that is, thermal equilibrium exists, then the total radiant energy from the sun is equal to the reflected radiant energy from the earth plus the energy radiating from the earth due to its temperature. For these assumptions the earth radiates as a black body having a temperature of approximately 454° R. This corresponds to an average radiant flux from the earth's surface of about 73 Btu/hr-ft^2.

Referring to Figure B-1 and using the Stephen-Boltzmann radiation law, the energy striking an element, dA, from the earth surface element, dS, is found from

$$dq = \frac{\epsilon\sigma T^4}{\pi} \frac{\cos\alpha \cos\dot{\eta}}{\rho^2} dS\, dA$$

where

$$\frac{\cos\alpha}{\rho^2} = \frac{(1+y)\cos\theta - 1}{\left[(1+y)^2 - 2(1+y)\cos\theta + 1\right]^{3/2} r_o^2}$$

$$\cos\eta = \frac{\left[(1+y) - \cos\theta\right]\cos\xi + \sin\theta \sin\xi \cos(\phi - \zeta - \delta)}{\left[(1+y)^2 - 2(1+y)\cos\theta + 1\right]^{1/2}}$$

$$dS = r_o^2 \sin\theta\, d\theta\, d\phi$$

The flux at a satellite surface point is

$$F = \frac{\epsilon\sigma T^4}{\pi} \int^{\theta}\int^{\phi} \frac{\left[(1+y)\cos\theta - 1\right]\sin\theta}{\left[(1+y)^2 - 2(1+y)\cos\theta + 1\right]^2} \left\{\left[(1+y) - \cos\theta\right]\cos\xi + \sin\theta \sin\xi \cos(\phi - \zeta - \delta)\right\} d\phi\, d\theta$$

Integration with respect to ϕ produces

$$F = \frac{\epsilon\sigma T^4}{\pi} \int^{\theta} \frac{\left[(1+y)\cos\theta - 1\right]\sin\theta}{\left[(1+y)^2 - 2(1+y)\cos\theta + 1\right]^2} \left\{\left[(1+y) - \cos\theta\right]\phi\cos\xi + \sin\theta \sin\xi \sin(\phi - \zeta - \delta)\right\}^{\phi(\theta)} d\theta$$

For the special case of a horizontal flat plate where

$$\xi = 0^{\circ}$$

the above equation may be further integrated mathematically with respect to the variable θ. In general, however, integration with respect to θ requires numerical methods.

Integration Limits of ϕ

The only limits imposed on ϕ are those due to the shielding effect of the satellite body itself as discussed in Appendix B.

The limits, as derived in Appendix B', are

$$\phi = \zeta + \delta \pm \left(\cos^{-1} \left\{ \frac{\left[(1 + y) - \cos \theta \right] \operatorname{ctn} \xi}{\sin \theta} \right\} - \pi \right)$$

Integration Limits of θ

The limit imposed on the angle θ is that corresponding to the earth horizon as viewed from the satellite.

$$\theta = \cos^{-1} \left(\frac{1}{1 + y} \right)$$

Elliptic Orbit

For an elliptic orbit the altitude varies with respect to the satellite orbit position. The substitution

$$1 + y = \frac{a(1 - e^2)}{r_o (1 + \cos \psi)}$$

as derived in Appendix B' must be made in the flux equation.

[redacted]

APPENDIX D'

DIRECT INSOLATION OF THE SATELLITE

The radiant energy flux due to direct insolation on an orbiting surface is given by

$$F = E \cos \beta'$$

The term $\cos \beta'$ is derived from Figure B'.3 as follows:

$\vec{z}$ = a unit vector lying along the z axis

$\vec{S}$ = a unit vector lying along a line joining the surface point to the center of the sun

$\vec{N}$ = a unit vector normal to the insolated surface

$$(\vec{z} \times \vec{S}) \cdot (\vec{z} \times \vec{N}) = \begin{vmatrix} \vec{z} \cdot \vec{z} & \vec{z} \cdot \vec{N} \\ \vec{S} \cdot \vec{z} & \vec{S} \cdot \vec{N} \end{vmatrix}$$

$$\sin \theta_S \sin \xi \cos(\delta + \zeta) = \cos \beta' - \cos \theta_S \cos \xi$$

Therefore,

$$\cos \beta' = \sin \theta_S \sin \xi \cos(\delta + \zeta) + \cos \theta_S \cos \xi$$

For an elliptic orbit,

$$\sin \theta_S = \cos \psi \cos \lambda - \sin \psi \sqrt{\sin^2 \Omega - \cos^2 \lambda}$$

as derived in Appendix B'.

$$\zeta = \sin^{-1} \left(\frac{\cos \Omega}{\sin \theta_S} \right)$$

as derived in Appendix B'.

The angles ξ and δ are derived from the particular satellite geometry for the surface point of interest. Thus,

$$F = E \left[\sin \theta_S \sin \xi \cos(\delta + \zeta) + \cos \theta_S \cos \xi \right]$$

[redacted]

There is always direct insolation on some part of the satellite except when the satellite is in the shadow of the earth. The limiting values of θ_S for the earth shadow are

$$90^\circ + \cos^{-1}\left(\frac{1}{1+y}\right) \leq \theta_S \leq 270^\circ - \cos^{-1}\left(\frac{1}{1+y}\right)$$

as shown in the following sketch:

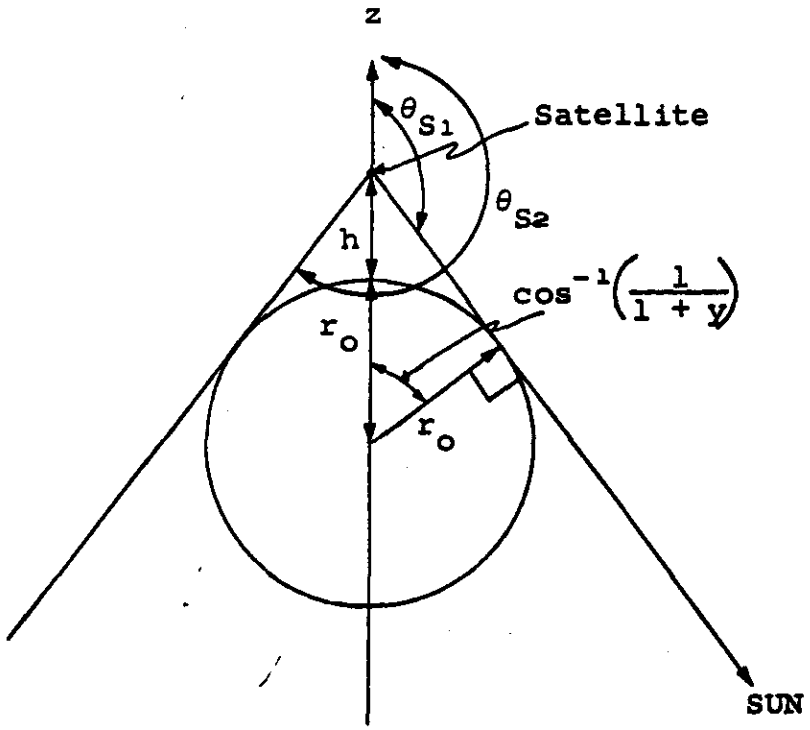

[redacted]

APPENDIX G

THE "J" SYSTEM SKIN TIME CONSTANT FOR RADIATION HEATING

The mean rate, averaged over the skin surface, of heat gain for the satellite skin is described by the differential equation

$$m\,c\,\frac{dT}{d\theta} = \alpha_s\,G_s + \alpha_A\,G_A + \epsilon\,G_e - \epsilon c T^4$$

where

- m the mass of a unit area of the satellite skin
- c the specific heat of the skin material
- α_s the solar abosrptivity of the skin
- α_A the albedo absorptivity of the skin
- ϵ the earthshine absorptivity and emissivity of the skin[1]
- G_s the instantaneous solar flux averaged over the skin surface
- G_A the instantaneous albedo flux averaged over the skin surface
- G_e the earthshine flux averaged over the skin surface
- c the Stephan-Boltzman radiation constant, 0.1713×10^{-8} Btu/hr-ft^2-$^\circ$R^4-ster
- T the instantaneous mean skin temperature
- θ time

This equation cannot be integrated mathematically for $\alpha_s G_s$ and $\alpha_A G_A$ being time dependent functions; ϵG_e is not time dependent. In order to obtain a time constant;

[1] This equality of the absorptivity and emissivity is explained in Appendix E.

[redacted]

that is, the time required for the skin temperature either to rise or fall to within $(1 - \frac{1}{e})$ of its steady-state value the orbital mean values of G_s and G_A will be used and the time required for the skin temperature to approach to within $(1 - \frac{1}{e})$ of its steady-state value will be computed. This period of time will be defined as the skin time constant.

Let

$$s^4 = (\alpha_s \bar{G}_s + \alpha_A \bar{G}_A + \epsilon G_e)/\epsilon \sigma$$

$$= \text{a constant}$$

The bars over G_s and G_A denote the use of the mean orbital heat fluxes. Then, the differential equation becomes

$$\frac{m c}{\epsilon \sigma} \frac{dT}{d\theta} = s^4 - T^4$$

Integration with respect to θ for $s^4 > T^4$ (that is, a heating situation) results in the equation

$$\theta = \frac{m c}{4 \sigma s^3} \left\{ \ln \left[\frac{(s + T)(s - T_o)}{(s + T_o)(s - T)} \right] + \left[2 \tan^{-1} \left(\frac{T}{s} \right) - 2 \tan^{-1} \left(\frac{T_o}{s} \right) \right] \right\}$$

where

T_o the initial skin temperature

T the skin temperature at time θ

For a $\beta = 40^\circ$ orbit the values used for the mean orbital heat fluxes averaged over space and time to a horizontal cylinder in a circular orbit having an altitude of 150 statute miles will be those presented in Appendix C, namely,

$$G_s = 69.3 \text{ Btu/hr-ft}^2$$

$$G_A = 16.4$$

$$G_e = 28.4$$

and for $\alpha_s/\epsilon = 1.086$ (as for "J-7") and the assumption that $\alpha_A = \alpha_s$

$$s^4 = \frac{1.086\ (69.3 + 16.4) + 28.4}{0.1713 \times 10^{-8}} = 709 \times 10^8\ {}^{\circ}R^4$$

This corresponds to an equilibrium temperature of $s = 516^{\circ}$ R.

The "J" systems have a mean-skin thickness of 0.070 inches; the skin material is magnesium having a density of 109 lbs/ft^3; the specific heat is 0.25 Btu/hr-lb-$^{\circ}$F at approximately 70° C (Ref. 9, p. 291 and 156).

Assuming an initial temperature of $T_o = 450^{\circ}$ R, the time required for the temperature to attain

$$450^{\circ}\ R + (1 - \tfrac{1}{e})\ (516^{\circ}\ R - 450^{\circ}\ R) = 492^{\circ}\ R$$

is from the above equation

$$\theta = 0.126 \text{ hours or } 7.6 \text{ minutes}$$

[redacted]

[redacted]

APPENDIX H

A QUALITATIVE EXPLANATION FOR THE DIFFERENCES FOUND TO EXIST BETWEEN THE MEASURED TRANSIENT SKIN TEMPERATURES AND THOSE COMPUTED USING A 130-NODE MATHEMATICAL MODEL OF THE SYSTEM

Temporal variations in the amount of earth-cloud cover cannot be used as a logical explanation for all the differences found to exist between the transiently computed temperatures of the "J-7" system and those measured. The differences found in the thermal analysis will be assumed, here, to be actual differences despite probable errors in the measured temperatures due to errors in the terperature sensor instrumentation and data read-out. Temporal variation in the extent of cloud cover should result in approximately the same difference between the computed and measured temperatures for both the barrel section and the conical fairing section of the system. However, for the hot side, the sun side, of the vehicle the actual or measured differences are of opposite sign, algebraically.

The Barrel Section

The accurate computation of the transient temperature of a portion of the vehicle skin is dependent upon the correct modeling of that portion's thermal mass (the product of the physical mass and the specific heat of the material) as well as the correct representation of the surface finish and the thermal environment. The mathematical relationship is shown in Appendix E.

[redacted]

SECRET

The masses of the skin nodes for the 130-node mathematical model of the "J" system were obtained by dividing the total mass of the vehicle skin plus the mass of the structural reinforcing component proportionally according to the skin nodal areas. This is approximately correct if the thermal conductance between the skin and these structural elements is sufficiently large to make the conductive heat-flow rate per unit temperature difference between them large compared to the radiation heat exchange between the space environment and the skin surface. For such a condition the entire nodal mass has approximately the same temperature throughout and the component elements of a node react as a unit. The heat input to the skin surface is effectively distributed through the entire nodal mass. This is the assumption made for the skin node modeling of the "J" system. Actually, however, there exists surface contact thermal resistance across the riveted and bolted joints between the structural reinforcing elements and the skin. As a result the actual combination of skin and structural elements do not react as a single thermal mass; the heat content variation of the node is largely confined to that portion of the node containing the exterior skin surface. A more accurate model would include the reinforcing structures as separate nodes with the appropriate thermal conductance between them and the adjacent skin nodes.

In the equation for the rate of temperature change (Appendix E) the rate is inversely proportional to the thermal

mass of the node. The larger the mass the smaller is the rate of nodal temperature change. When the assumed thermal mass for computing purposes is larger than that actually existing in the hardware the computed rate of nodal temperature change will be less than that which actually exists. Therefore, for a given radiation environment which varies periodically with time the computed nodal temperature will always lag the measured temperatures. During the heating portion of the cycle the measured temperatures will be higher than those computed; during the cooling portion of the cycle the measured temperatures will be lower than those computed. An excellent example of this is presented in Figure 6 of Reference 2.

The effects of these errors in the transient temperatures of the barrel skin upon interior temperatures are quite small. The mean skin temperature which controls the mean interior temperature does not depend upon the numerical values of the skin-node masses as is; this is shown by the equations of Appendix E. Also, the amplitudes of the temperatures of the instrument main plates are approximately 3° F (Ref. 2, Fig. 9); a 100 percent error in the amplitude of the barrel skin temperature could cause no more than a 3° F error in the amplitude of the temperatures of the instrument main plates; this is only 1/3 of the temperature range tolerance, $\pm 10^{\circ}$ F. From Figure 6 of Reference 2, the difference in the computed from the measured amplitude of node 96 is less than 35 percent; thus the error in the instrument temperature amplitude

is probably on the order of 1° F, and is, in the light of the above range tolerance, negligible.

The Fairing Section

The fairing or conical section of the "J" system was modeled in the same manner described above for the barrel section. However, the mathematical model does not include the first recovery unit of the system and that unit's influence upon the fairing temperature is not accounted for[1]. That unit has an ablative, reentry shield that joins the conical skin section. The ablative material, a plastic, is not coated with the thermal paint mosaic and has a different radiant energy absorptivity, α, and emissivity, ϵ, than that for the rest of the vehicle. The value of the α/ϵ given for a representative ablative material in Reference 10, p. F-57, is about 0.51/0.75 or about 0.68. This value, being less than 1.0, will result, according to the equations of Appendix E, in a recovery unit temperature that is below that of the fairing. From Vidya Division's thermal library, the radiation heat fluxes to a 15° cone for a β = 40° orbit result in the mean orbital heating fluxes, solar plus albedo, and earthshine of

$$\bar{G}_S + \bar{G}_A = 83.7 \text{ Btu/hr-ft}^2$$

$$G_e = 28.0$$

and, using the equation of Appendix E,

$$\epsilon \overline{T^4} = \frac{\alpha}{\epsilon} (\bar{G}_S + \bar{G}_A) + G_e$$

$$\left(\overline{T^4}\right)^{\frac{1}{4}} = 472° \text{ R} \quad \text{or} \quad 12° \text{ F}$$

[1] Computations performed by Vidya Division using the 130-node model indicate that a 15° F variation in the mean temperature of the fairing section results in an instrument main plate temperature variation of less than 3° F.

[redacted]

This would represent the orbital mean temperature of the external surface of the ablative material. Thus, this ablative section can be expected to lower the temperature of the fairing by thermal conduction through the structural elements uniting the two sections. The measured temperature for the interior of the first recovery unit is about 42° F (Appendix A); the thrust cone of this unit has a measured temperature of about 45° F (Appendix A). These higher interior temperatures result from the active heating used in this section and from the heat transfer from the fairing section to the first recovery unit. Therefore, the measured mean temperatures of the fairing section of the vehicle can be expected to be lower than those computed. However, the measured transient temperatures are functions, also, of the nodal masses as described above for the barrel section. The model, having thermal masses that are larger than the actual reactive thermal masses of the system may for some assumed thermal environments result in temperature predictions that are lower than those measured. Without modeling the first recovery unit and the fairing skin structural components the algebraic sign of the results compared to that for the measurements for the fairing skin cannot be predicted since the measured mean temperature, low because of the thermal influence of the first recovery unit, may or may not be sufficiently low compared with the computed value to maintain the fairing transient temperature amplitude extremes below the maximum or above the minimum values of the computed transient temperatures.